NASA

Technical Memorandum 80336

Characterization of the Q-Switched MOBLAS Laser Transmitter and its Ranging Performance Relative to a PTM Q-Switched System

John J. Degnan
Thomas W. Zagwodzki

OCTOBER 1979

National Aeronautics and Space Administration

Goddard Space Flight Center
Greenbelt, Maryland 20771

CHARACTERIZATION OF THE Q-SWITCHED MOBLAS LASER TRANSMITTER AND ITS RANGING PERFORMANCE RELATIVE TO A PTM Q-SWITCHED SYSTEM

John J. Degnan
Thomas W. Zagwodzki

October 1979

GODDARD SPACE FLIGHT CENTER

Greenbelt, Maryland

Page intentionally left blank

CHARACTERIZATION OF THE Q-SWITCHED MOBLAS LASER TRANSMITTER AND ITS RANGING PERFORMANCE RELATIVE TO A PTM Q-SWITCHED SYSTEM

John J. Degnan
Thomas W. Zagwodzki

ABSTRACT

This report documents the results of various tests performed on a prototype Q-switched Nd:YAG laser transmitter intended for use in the NASA mobile laser (MOBLAS) ranging stations and various modifications of the basic laser. The tests were designed to determine temporal pulseshape and stability, output energy and stability, beam divergence, and most importantly, the range bias errors introduced by the transmitter. Based on the results of each phase of testing, the system was modified and reevaluated with regard to its ranging performance over a fixed horizontal range. The basic system consisted of a simple Q-switched oscillator followed by a double-pass amplifier and KD*P Type II frequency doubling crystal. The pulse width of the Phase I oscillator was six nanoseconds (FWHM), but the laser introduced large biases which varied both in time and with the location of the target in the transmitter far field pattern. Peak-to-peak variations in the mean range (for sets of 100 individual range measurements) were as large as 30 cms (±15 cm). The Phase II oscillator pulsewidth was reduced to 4 nsec (FWHM), but the peak-to-peak variation in the mean range was still on the order of 18 cms. A typical drift rate of the system bias with time was 6 mm per minute of operation. A fast electro-optic cavity dump with a subnanosecond risetime was incorporated into the final Phase III oscillator. The resulting pulsewidth was 1.5 nanoseconds (FWHM), and the peak-to-peak variation in the mean range was reduced to the two to three centimeter level. A qualitative physical explanation for the superior performance of cavity dumped (also called PTM Q-switched) lasers is given.

Page intentionally left blank

CONTENTS

CHARACTERIZATION OF THE Q-SWITCHED MOBLAS LASER TRANSMITTER AND ITS RANGING PERFORMANCE RELATIVE TO A PTM Q-SWITCHED SYSTEM

I. Introduction

Since the first successful satellite laser ranging system was demonstrated at the Goddard Space Flight Center in 1964, the error in the range measurement has decreased dramatically from several meters in 1964 to less than 10 cm by 1975.[1] In 1975, the Goddard Laser Tracking Network consisted of one fixed station and three mobile units and at the present time is being expanded to include five additional mobile units with ranging capability on the order of 5 to 10 cms. Several of the key components in these new systems are different from those used in the earlier successful prototype ranging systems. One such component is the laser transmitter itself.

The prototype mobile systems used Q-switched and cavity-dumped ruby laser oscillators built by the Korad Corporation, which produced quarter-joule pulses with a full-width, half maximum pulsewidth (FWHM) of four nanoseconds. Since ruby is a three-level laser system it requires large pump energies to achieve threshold. The material Nd:YAG, on the other hand, is a four-level system which achieves threshold at significantly lower pump energies and was therefore selected as the laser medium for the new ranging systems. The new transmitters, built by General Photonics, consist of a Q-switched Nd:YAG laser oscillator, followed by a double-pass Nd:YAG laser amplifier, and a KD*P-Type II doubling crystal. The latter component converts the 1.064 micrometer infrared wavelength of Nd:YAG to the 0.532 micrometer green wavelength used by the ranging receiver. The pulsewidth of this new laser was about six nanoseconds (FWHM)-only slightly longer than the Q-switched, cavity-dumped ruby output in the successful prototype systems.

Historically, it is important to note that highly unsatisfactory ranging performance had been observed in early ruby systems when the laser oscillator was Q-switched but not cavity-dumped. These early systems were characterized by poor repeatability in the range measurement to a fixed target retroreflector and by biases determined by the angular position of the target in the far field

illumination pattern of the transmitter. Admittedly, the pulsewidths of these early Q-switched systems were significantly longer (20 nanoseconds), but this in itself would not be sufficient to explain the angular dependence of the range measurement. It was postulated that the angular dependence of the range measurement was due to the fact that, since different transverse modes have different buildup times in the resonator (due to different losses) and different radiation patterns in the far field (higher order modes diffract over a wider far field angle), the temporal profile seen at the target will vary with its position in the far field pattern. The ranging difficulties associated with this phenomenon were first alleviated by the use of an external electro-optic switch to slice a 5 nanosecond segment out of the 20 nanosecond Q-switched ruby pulse and later by the incorporation of a cavity dump internal to the laser oscillator. This concept will be explored in more depth later in this report.

In any event, it seemed prudent to test the new General Photonics laser as part of a ranging system under controlled laboratory conditions prior to its installation in the new mobile systems, which were intended for immediate field use.

The system was shipped to Goddard in May, 1978, for testing and evaluation. These tests, hereafter called Phase I, were designed to fully characterize the laser and verified that, in the laboratory ranging system, the new laser exhibited many of the detrimental characteristics of the earlier Q-switched ruby lasers. In addition, there was strong evidence of mode-locking or longitudinal mode-beating effects which resulted in non-stationary temporal profiles and poor repeatability in the range measurement. Our principal recommendations at the completion of the Phase I tests was the incorporation of a cavity-dump in the laser oscillator.

A slightly modified version of the system was returned for testing in September, 1978. The principal innovation was a shorter cavity length which produced a 4 nanosecond pulse width (FWHM). While some small improvement in ranging performance was observed, the ranging error introduced by this Phase II laser was still unacceptably large.

In December, 1978, a cavity-dump was incorporated into the General Photonics Laser and the system was returned for a third testing sequence hereafter referred to as Phase III. Preliminary results indicated a marked improvement in the repeatability of the range measurement but the ranging

data still exhibited a strong angular dependence. Subsequent experiments indicated that the rise time of the cavity-dump switch supplied by the contractor was too slow. The switching circuitry was replaced by an in-house design with a very fast rise time (<1 nanosecond). The resulting pulse-width was 1.5 nanoseconds between the half-maximum points and about three nanoseconds at the base. The range results were highly repeatable and did not exhibit the angular biases observed during the earlier test sequences.

The present report documents testing procedures and results obtained during Phases I through III in the hope that it will be useful to present and future contractors and to other parties with an interest in precise laser ranging.

II. Temporal Pulseshape and Stability

A temporal pulseshape which varies significantly from shot to shot can cause large random errors in a laser ranging system. For this reason, the stability of the General Photonics laser temporal profile was investigated. For the sake of redundancy, a variety of subnanosecond detectors including (1) a Sylvania Model 502 Photomultiplier (2) a Varian Model VPM-154 A/1.6L Static Crossed Field Photomultiplier, (3) a Monsanto MD2 Photodiode, and (4) an ITL (Instrument Technology Limited) S-20 photodiode were used. The bandwidth of the detection system was limited to 500 MHz by the Tektronix R7912 waveform digitizer which was used to display the pulseshape. The waveform digitizer was interfaced with a DEC PDP-11/40 minicomputer. Software developed previously allowed the display of one or more stored waveforms on a CRT display. The software also permits the display of an average waveform obtained by storing a preselected number of individual waveforms within the computer, summing them, and dividing by the total number of waveforms. Selected hard copies of the CRT display could be obtained via keyboard commands to an on-line printer.

The full power from the laser was first attenuated by means of neutral density filters. The latter were placed at skewed angles in the beam in order to avoid multiple reflections which might distort the measured pulseshape. The green radiation was then isolated from the infrared radiation via an infrared blocking filter. Sufficient additional attenuation was provided to avoid saturation of the detector. A block diagram of the experimental apparatus is illustrated in Fig. 1.

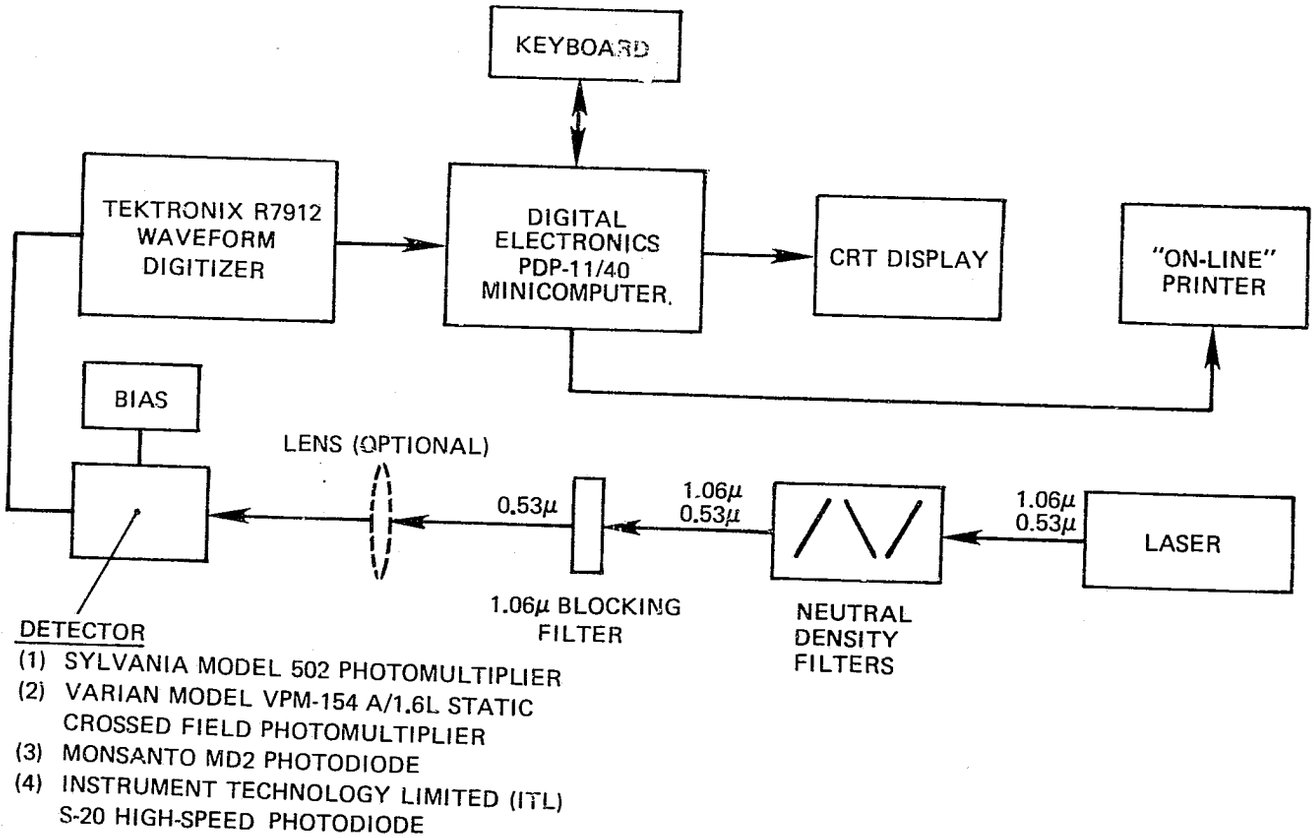

Figure 1. Experimental Apparatus for the Measurement of the Pulse Temporal Profile

The results obtained were independent of the choice of photodetector. In each and every case, the pulseshape was observed to vary between a rather smooth 6 to 7 nanosecond (FWHM) profile and a strongly modulated shape having several peaks but still following the basic six to seven nanosecond envelope. Examples of a smooth, moderately modulated, and strongly modulated waveform are illustrated in Figs. 2(a) through 2(c) respectively. Most pulses were moderately modulated although smooth and strongly modulated pulses appeared quite frequently in the pulse train. In these measurements, virtually all of the beam cross-section was sampled. In some cases, the beam was focused onto the detector, and, in other cases, it was not. The same results were obtained with either method of detection. The variation in pulse shape was usually dramatic from shot to shot as evidenced by Fig. 3(a) through 3(c) which shows several superimposed waveforms taken, not successively, but within several seconds of each other.

Adjacent peaks in the modulated pulses were separated by a time interval of slightly more than two nanoseconds which corresponds to the approximate round-trip resonator transit time. The latter observation indicates that random self-modelocking or longitudinal mode-beating is taking place in the cavity. Very rarely, a modulated pulse with peaks separated by only one nanosecond, corresponding to the one-way cavity transit time, was observed as in Fig. 4. Such behavior has been known to occur in passively modelocked lasers when two oppositely-traveling modelocked pulses are circulating in the cavity.

In spite of the strong modulation, the average waveform is quite stable and corresponds to a rather smooth Q-switch waveform with a six to seven nanosecond (FWHM) pulsewidth as in Fig. 5. At no time during these near field measurements, in which the total beam cross-section was sampled, did we observe pulsewidths longer than six or seven nanoseconds. In Section VI, however, we will present evidence that it is possible to receive much longer pulses from a small retroreflector target in the far field when certain pointing errors are introduced into the range link.

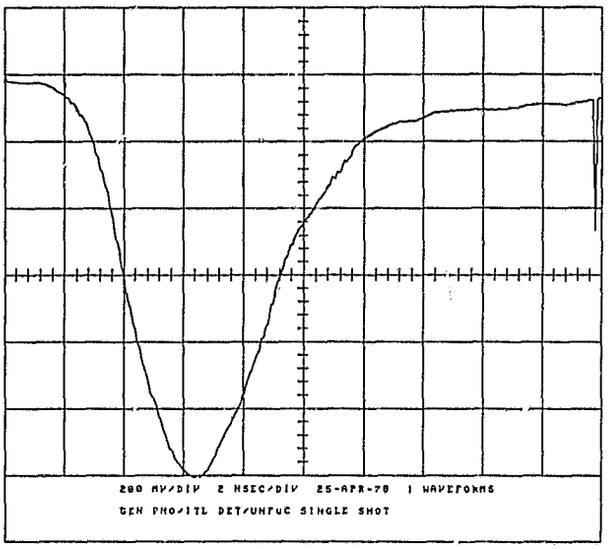

Figure 2(a). A Smooth Q-switched Pulse from the General Photonics Laser Observed with an ITL Photodiode and Tektronix R7912 Waveform Digitizer

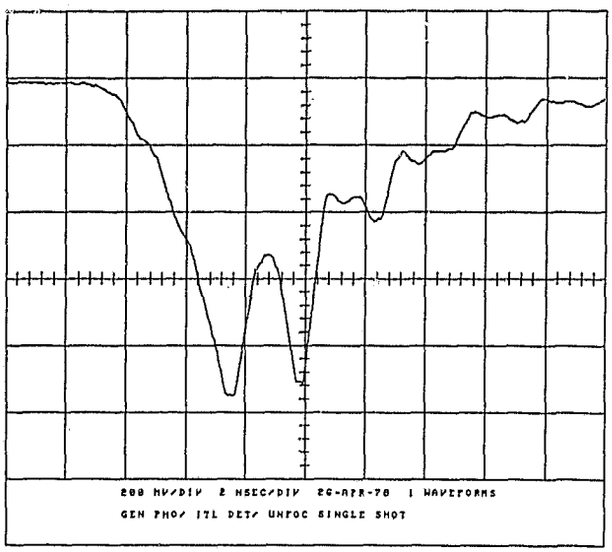

Figure 2(b). A Moderately Modulated Pulse from the General Photonics Laser Observed with an ITL Photodiode and Tektronix R7912 Waveform Digitizer

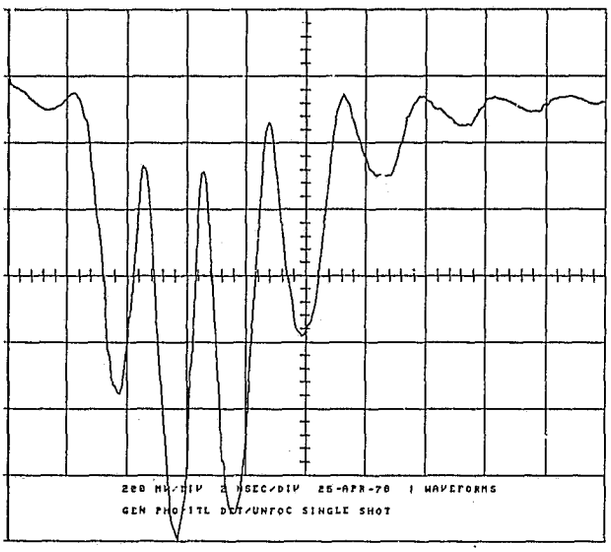

Figure 2(c). A Strongly Modulated Pulse from the General Photonics Laser Observed with an ITL Photodiode and Tektronix R7912 Waveform Digitizer. The Time Interval between Self-Modelocked Pulses is Approximately Two Nanoseconds Corresponding to the Oscillator Roundtrip Transit Time.

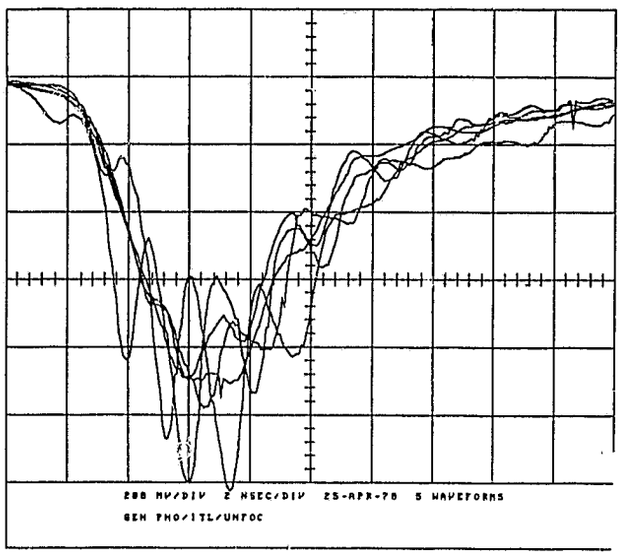

(a)

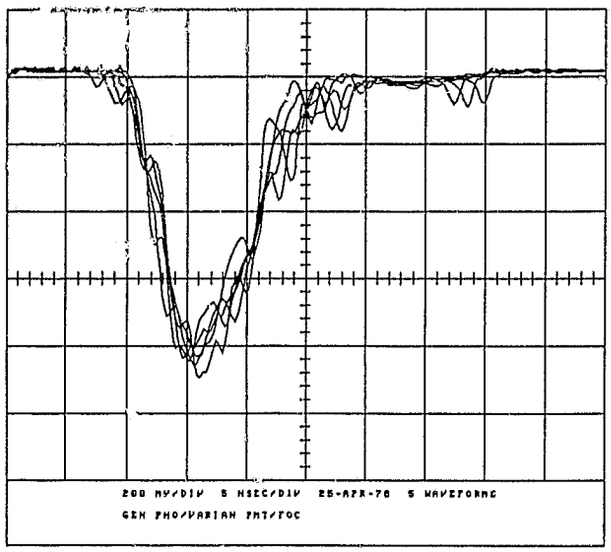

(b)

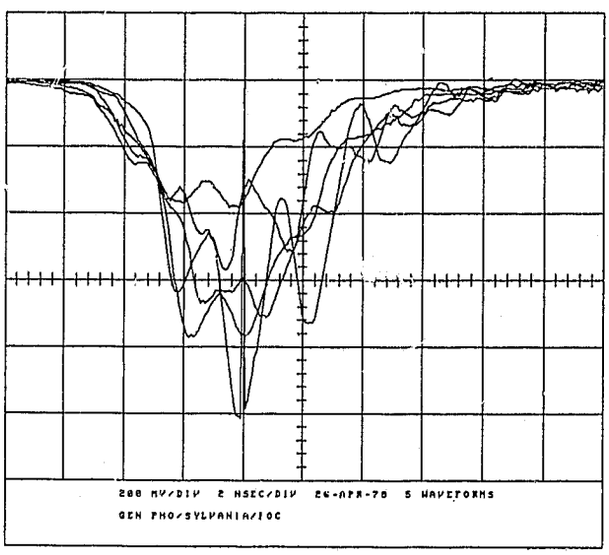

(c)

Figure 3. Five sample waveforms taken over three separate 30 second intervals with (a) The ITL Photodiode, (b) The Varian Photomultiplier (5 nsec time scale) and (c) The Sylvania Photomultiplier.

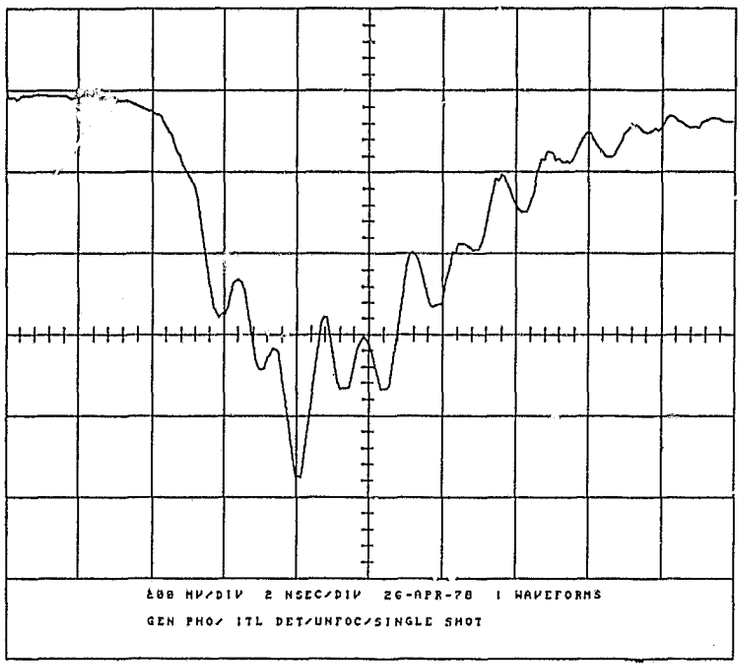

Figure 4. Waveform Exhibiting One Nanosecond Time Intervals between Adjacent Peaks and Indicating the Presence of Two Oppositely Directed Modelocked Pulses Circulating in the Oscillator Cavity.

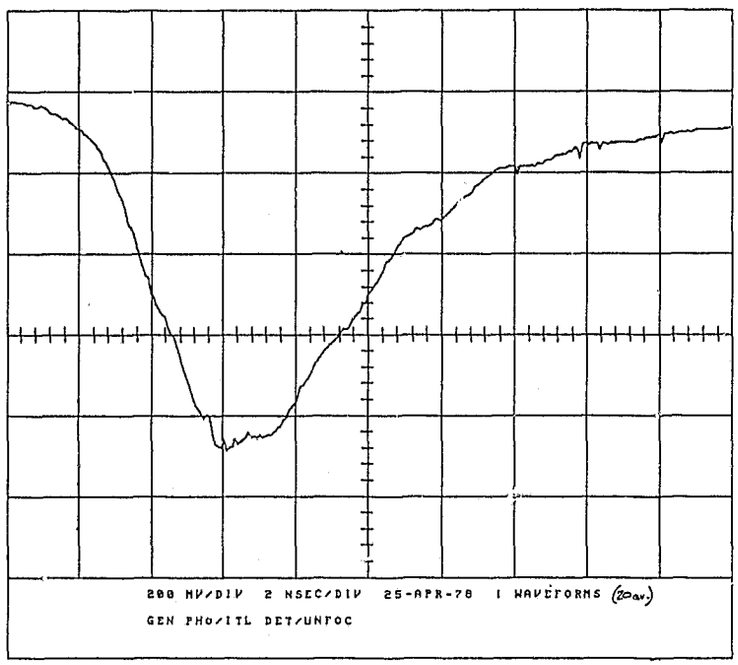

Figure 5. Average of Twenty Pulseshapes Observed with an ITL Photodiode and Tektronix R7912 Waveform Digitizer

III. Output Energy and Stability

Measurements were made of the total output energy and of the green energy from the laser. As with the pulse profile measurements, the energy measurements were normally made after completion of the field alignment p- edure as outlined in the General Photonics Technical Manual for the Model Two-80 YAG system. The total energy was measured directly with a Quantronix Model 504 Energy-Power Meter in conjunction with a Quantronix Model 501 Energy Receiver. Ten shots were selected from the 1 pps pulse train by an electronically controlled mechanical shutter, and the average pulse energy was computed. For the measurement of the green energy, a 1.06μ blocking filter ($<<1\%$ transmission) was inserted in the beam path. The filter transmission at 0.53μ was measured to be 65%. A block diagram of the absolute energy measurement apparatus is shown in Fig. 6.

Following the standard field alignment procedures as outlined in the technical manual, a total output energy of about 500 mJ could usually be achieved. A history of the day-to-day output energy is shown in Fig. 7. The peak output energy of 530 to 560 mJ was observed early in the test period shortly after a General Photonics technician had completed a refurbishing and complete alignment of the system. One month later, a total output energy of 495 mJ was obtained. The minimum output energy on any given test day was 430 mJ.

The day-to-day variation in green energy was somewhat more severe, and we believe that this was due to the degree of longitudinal mode-beating in the system. For total pulse energies of 500 mJ, one could usually achieve between 210 and 270 mJ of green energy following the alignment procedure outlined in the General Photonics Technical Manual.

Pulse-to-pulse energy stability of the green radiation was monitored using the experimental apparatus in Fig. 8. The beam was attenuated using neutral density filters and passed through the 1.06μ blocking filter into a Laser Precision Model RKP-335 (Option RF) Pyroelectric Energy Probe which was read by a Laser Precision Model RF3232 Energy Ratiometer. The latter instrument, which was equipped with a BCD output plug, was interfaced with the PDP-11 minicomputer. The pyroelectric probe is capable of measuring individual pulse energies at repetition rates up to 30 pps. Software provides a CRT display of the pulse-to-pulse energy stability and/or an energy histogram. Hard copies can be obtained using the on-line printer.

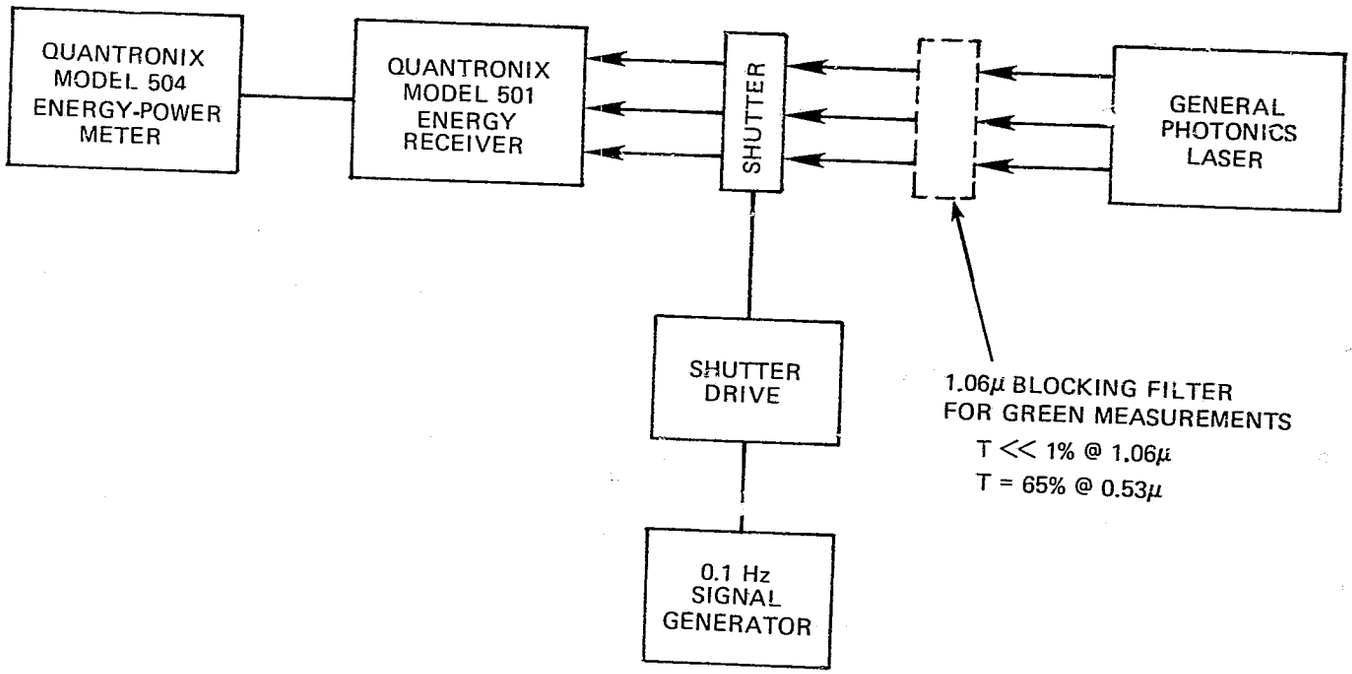

Figure 6. Experimental Apparatus for Absolute Energy Measurements

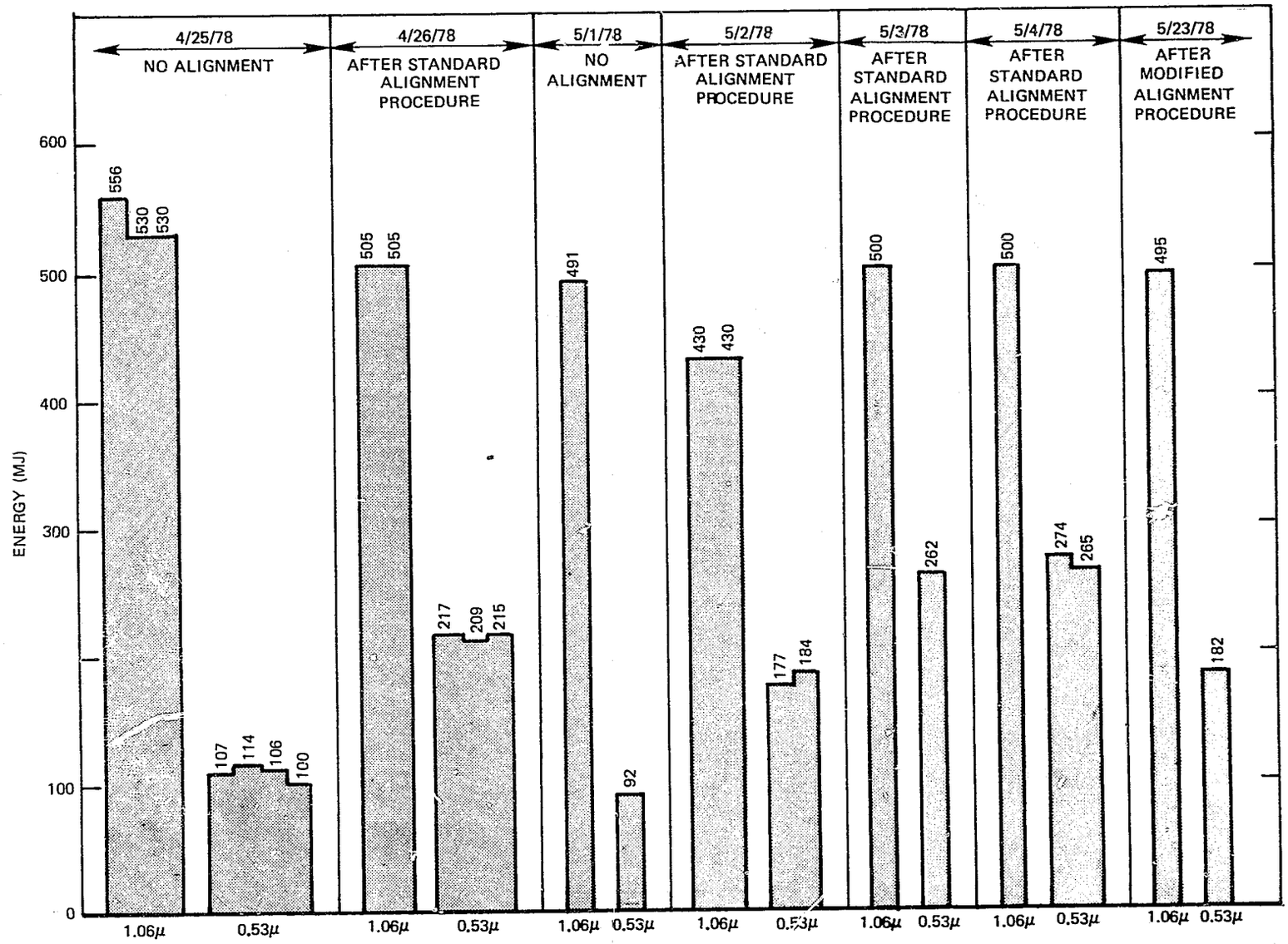

Figure 7. Total and Green Energy Output on Arbitrary Days during Laser Test Period

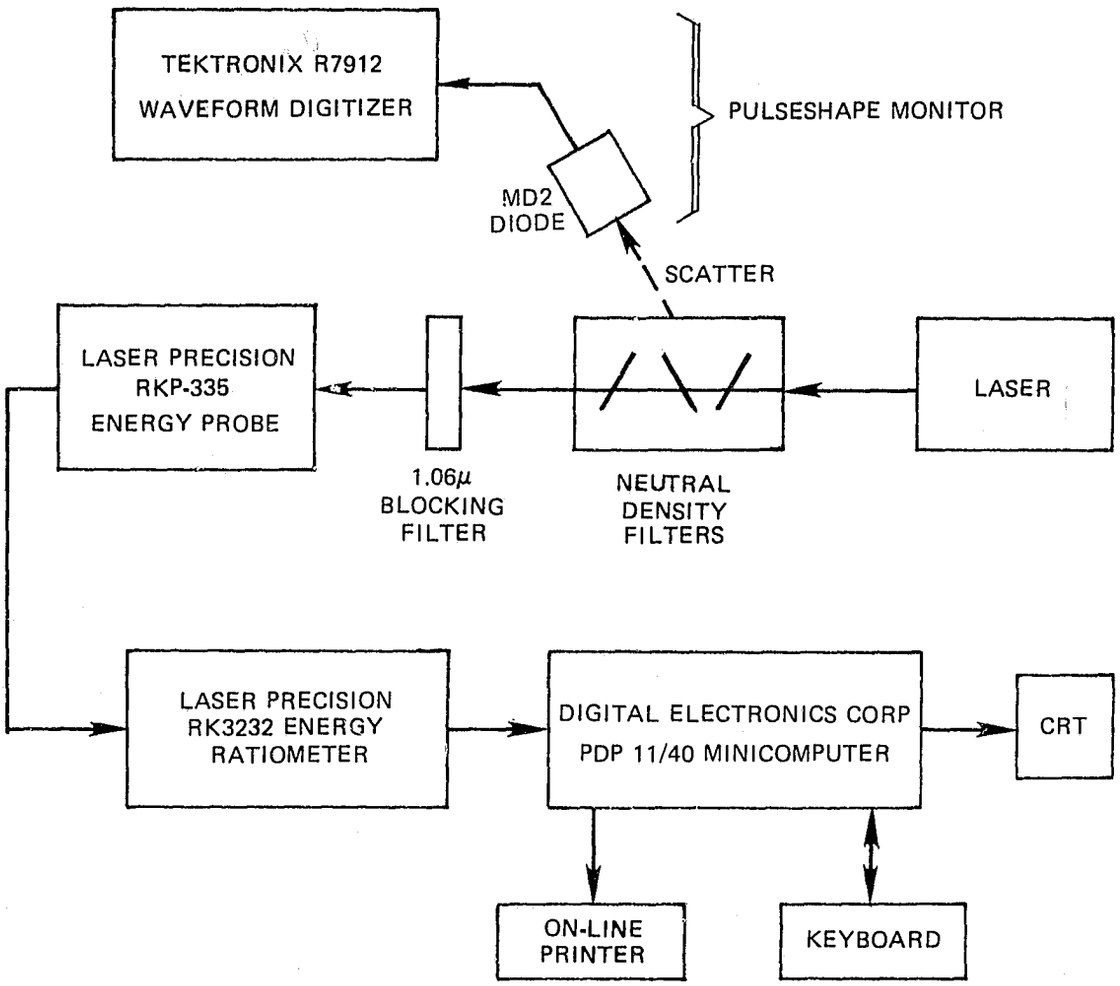

Figure 8. Experimental Apparatus for Measuring Stability of Green Output Energy

In less than a minute after turn-on, the General Photonics Model Two-80 System reaches its steady state energy as demonstrated in Figure 9(a). The latter figure, which is characteristic of a large number of data sets on energy stability taken during the test period, indicates a pulse-to-pulse energy stability of about ±4% in the steady state. This particular data set was taken on the morning of April 26, 1978, following the standard field alignment procedure. The system was turned off during the lunch hour, and, upon being turned on again, the pulse energy exhibited the erratic behavior in Figure 9(b). In the latter state, the green energy oscillated between two levels. By simultaneously monitoring the output with a fast detector, it was determined that the high green energy state was associated with pronounced self-modelocking effects in the oscillator as illustrated in Figure 2(c), while the low green energy state was associated with smoother profiles as in Figure 2(a). Generation of the second harmonic is more efficient for the mode-locked pulses because of their significantly higher peak intensities relative to the smoother, Q-switched profiles. While Figure 9(b) represents a possible operating state, Figure 9(a) is much more typical of the pulse energy stability data.

As a result of the data in Figure 9, it was felt that the field alignment procedure, in which one peaks the green output by alternately adjusting the oscillator and doubling crystal alignment, might tend to force the oscillator into a self-modelocked state since the latter condition favors high green output. An alternate alignment technique was therefore implemented in which the oscillator was aligned for maximum total output energy and the doubling crystal was then aligned for maximum green energy. Contrary to the normal procedure, the oscillator alignment was not adjusted further. The energy obtained on May 23, 1978, using this alternate alignment technique, is included in the data of Figure 7. The total output energy of 495 mJ is comparable to earlier data, but the green energy per pulse is significantly less than that obtained using the conventional alignment procedure (182 mJ vs. 260 mJ). It was observed that, although the second harmonic pulse profiles were smoother on the average, the presence of self-modelocking was still quite evident even at these lower green energies. Furthermore, the choice of alignment procedure seemed to have little or no effect on the quality of the ranging data to be described in Section VI.

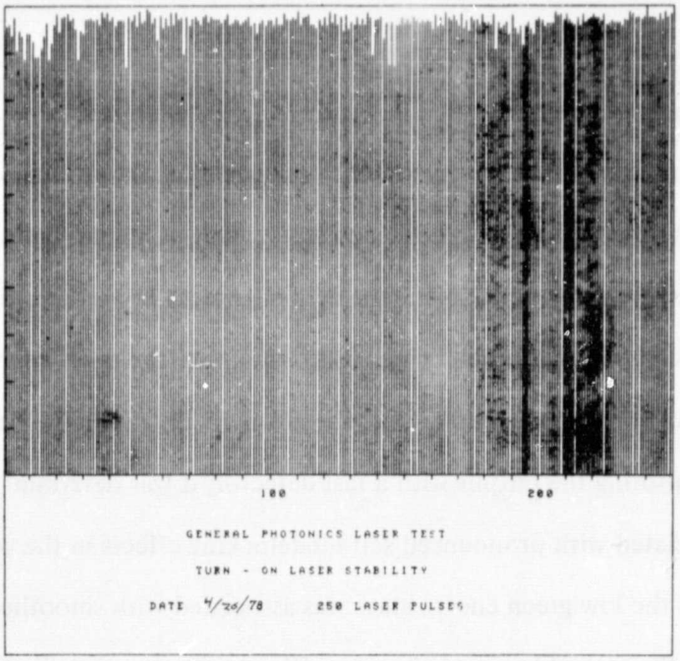

Figure 9(a). Pulse-to-Pulse Green Energy Stability Following Normal Field Alignment Procedure

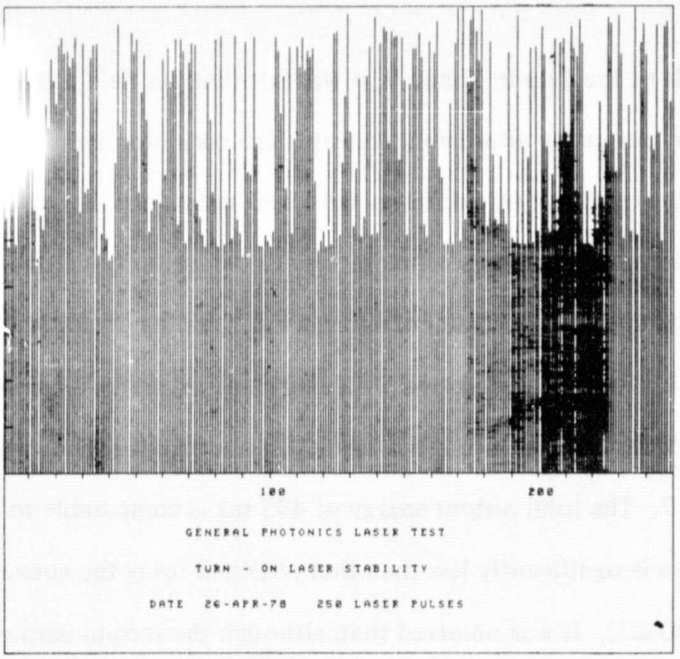

Figure 9(b). Pulse-to-Pulse Green Energy Stability after Two Hour Shutdown, Oscillator is switching between Strongly Mode-locked Profile and Smooth Q-switched Waveform

IV. Beam Divergence

The experimental configuration for the measurement of beam divergence is illustrated in Fig. 10. The output beam was reflected from two high surface quality dichroic mirrors which reduced the 1.06 micrometer content (via transmission) to about 1% of its initial value. Approximately 97% of the 0.53 micrometer radiation was reflected off the second dichroic and focused onto a variable aperture pinhole by a lens having a focal length of 309.7 ± 1.0 cm. In order to avoid damage to the pinhole, the beam intensity had to be attenuated. Surface coating damage of metallic reflective attenuators ruled out their use, while absorbing attenuators were questionable due to unknown divergence effects from beam-induced thermal lensing. The beam was attenuated, therefore, by reflecting the light off two prism faces. Prisms were chosen over flat plates to avoid multiple parallel beam effects which would invalidate the divergence measurements.

The final low level beam was passed through a 1.06 micrometer blocking filter to eliminate any residual infrared energy. The focused spot was then centered on the variable pinhole, and measurements were made of the transmitted energy as a function of pinhole diameter. The pinhole diameters were accurately measured with calipers. The energy reading was taken using the pulse averaging circuitry on the Laser Precision Model RK3232 Pyroelectric Energy Ratiometer which allows an average of 10 shots at 1 pps. The diameter of the pin hole is related to the far-field angle α by the relationship

$$\alpha = D/f$$

where f is the focal length of the lens. The results of the measurements are plotted in Fig. 11 where it should be noted that 90% of the far field energy is contained in a cone of revolution with a full apex angle of 0.68 mrad. Thus, with the final 4.2 power collimator properly focused, 90% of the energy will be contained within a 0.16 mrad cone.

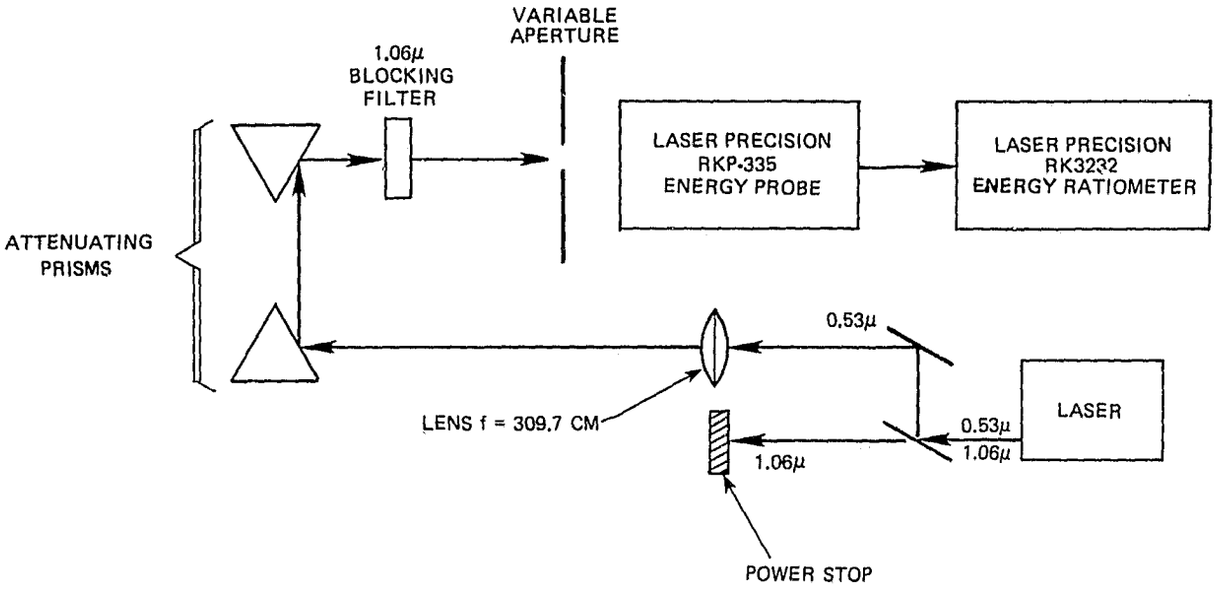

Figure 10. Experimental Apparatus for the Measurement of Laser Beam Divergence

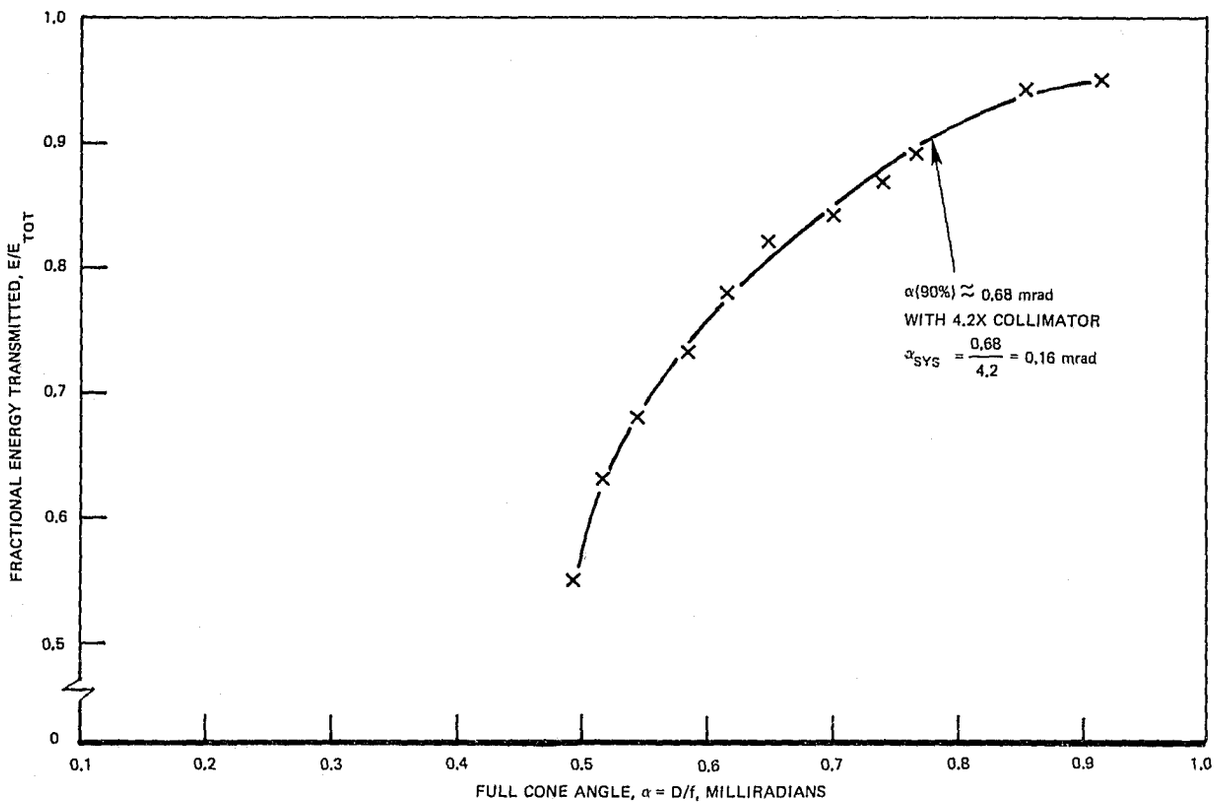

Figure 11.

V. Phase I Range Receiver Description and Calibration

The careful characterization of the receiver independent of the laser transmitter is required to determine the level of timing error it contributes to the range measurements. Only then can the ranging errors attributable to laser effects be isolated from those contributed by the receiver. The receiver used in all range measurements was designed specifically for the General Photonics Laser. Recently developed laboratory test techniques have allowed for individual receiver component testing as well as whole receiver system evaluation.[2] Final range receiver configuration was decided upon after extensive testing and optimization for a 6 to 8 nanosecond (FWHM) laser pulse. This receiver evaluation work was required to minimize the effect of receiver uncertainty in range measurements.

Shown in Figure 12 is the best range receiver configuration that was available at the time of testing. Individual receiver components used in the system had been tested and characterized prior to the General Photonics tests. The start channel is triggered by a .5 nanosecond rise time (10%-90%) Monsanto MD2 silicon photodiode. The diode was physically positioned to trigger on a back reflection off a neutral density filter in the outgoing transmitted laser pulse. Since the timing electronics cannot trigger reliably when the triggering pulses have differing or random structure as was observed in the General Photonics laser, a 300 MHz low pass filter was inserted to eliminate any structure within the outgoing laser pulse. Later tests showed a ranging residual improvement when the low pass filter was included while laser pulse structure was present. A similar low pass filter (200 MHz) was used in the stop channel. The positive-going diode start output was inverted using an EG&G inverting transformer prior to triggering the timing discriminator. An ORTEC model #473A constant fraction discriminator was used to minimize timing errors due to laser amplitude fluctuations. With electrical attenuation (3 db) and precise positioning of the diode, the discriminator pulse input level was set at 500 mv. This level is the logarithmic mid-point of the discriminators 40 db operating range, and the best operating point from the standpoint of discriminator time walk. Two to one amplitude variations (as observed in modelocking) map into less than ±50 picoseconds timing error. Laser amplitude stability as shown in Figure 9(a) maps into approximately ±10 picoseconds. Discriminator output is a −800 mV, 10 nanosecond width pulse which triggers the start channel of the Hewlett Packard HP5360

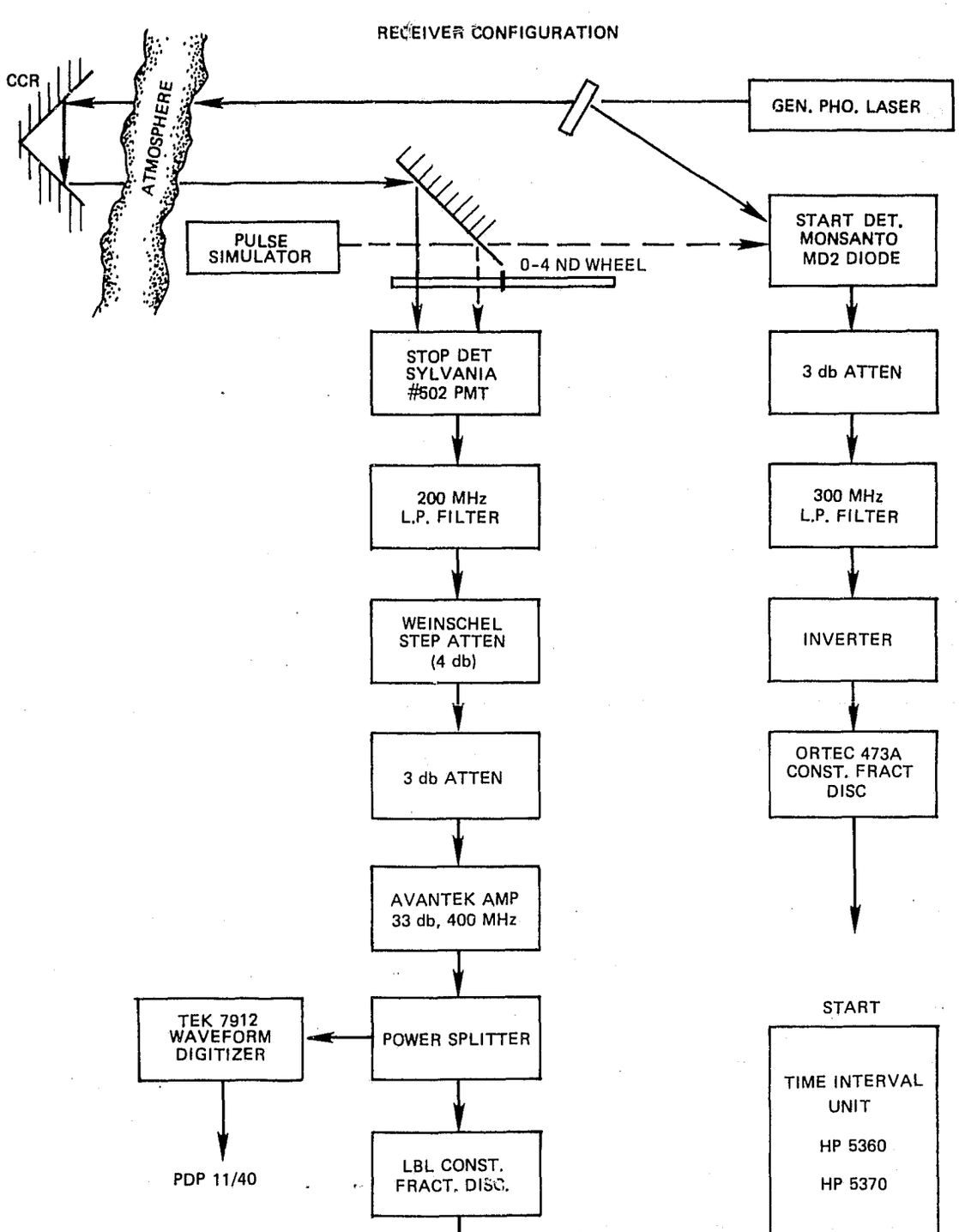

Figure 12. Phase I Receiver Configuration

or HP5370 Time Interval Unit (TIU). The HP5360 TIU and Tektronix R7912 waveform digitizer are interfaced to a Digital Electronics Corp. PDP 11/40 minicomputer for data taking and storage as well as statistical analysis.

The stop channel timing components will now be discussed. The transmitted laser pulse, after being returned by the cube corner reflector and laboratory periscope/telescope system (to be described in Section VI), is collimated and brought to a focus on a Sylvania Model 502 static cross field photomultiplier tube (PMT). The Sylvania PMT has a rise time (10%-90%) of less than 150 picoseconds and low time jitter (less than 30 picoseconds). The PMT output was filtered, as mentioned earlier, with a 200 MHz low pass filter to eliminate subnanosecond structure within the return pulse. Average electrical signal levels were maintained in the optimum range using an adjustable attenuator and fixed amplifier. A fixed 3 dB Weinschel attenuator along with a variable 0-60 db Weinschel step attenuator Model #AE177A-69-34 was used. The amplifier was an Avantek Model #AV-8B with 33 dB gain and 400 MHz bandwidth. The negative going signal is split to provide a voltage monitoring point for the discriminator input. A Tektronix R7912 waveform digitizer was used here to monitor and record return signal waveforms. Two timing discriminators were found necessary for the receiver to perform adequately. The first timing discriminator in the stop channel was a Lawrence Berkeley Laboratory (LBL) constant fraction discriminator which was designed for operation on a 5 nanosecond FWHM pulse. This discriminator was found to work acceptably well with a 6-8 nanosecond FWHM pulse. Although the full 100-1 dynamic operating range showed considerable time walk (approximately ±1 nanosecond) a 45 to 1 dynamic range produced only ±130 picoseconds time walk and a 7 to 1 range (which applied to most data) translated into only ±30 picoseconds time walk. A slight dependence of LBL discriminator output width on the input pulse amplitude was found. This varying width trigger pulse introduced time biases within the HP5360 TIU. To eliminate this time dependence, a second discriminator, an ORTEC Model 473A, was used. In this configuration, the superior time walk characteristics of the LBL discriminator could be used without introducing the timing error in the HP5360. The second discriminator contributes virtually no time walk (due to the constant input amplitude) and negligible time jitter (measured in the 5 to 10

picosecond range). To assure the best possible receiver performance the average stop pulse amplitude was continuously monitored and maintained at the 500 mV level using the variable optical attenuator wheel (0 to 4 ND) shown in Figure 12. As we will soon demonstrate, operation in this range utilized the flattest portion of the discriminator characteristic time walk curve. Data on receiver performance will be presented after receiver calibration has been discussed. All of these optimizations were made to assure ourselves that receiver effects in observed range data anomalies were minimized. The extent of receiver error will now be quantified.

Since time walk due to signal amplitude fluctuations and receiver system time drift may be the dominant error sources in this ranging receiver, a careful measurement of these effects is required. Conducting these tests under controlled laboratory conditions without atmospheric effects permitted precise calibration to the picosecond level.

Several calibration techniques were used to characterize the ranging system performance. All techniques involve time interval averaging of system delay of the receiver using the HP5360 or HP5370 TIU. The first of these was an electrically generated (E&H Model 129 Pulse Generator) pair of start and stop pulses similar in rise time and pulse width to ranging pulses. Using a Weinschell step attenuator on the stop side, system delay was accurately measured at each 1 db step change in receiver pulse amplitude. The resulting time walk curve shown in Fig. 13 represents an average over 50 time delay measurements for each 1 db attenuation step. The vertically dashed lines are the operating limits of the discriminator (50 mV to 5 volts). All data is referenced to the system time delay at 500 mV, the logarithmic mid-point of the discriminator operating range. As can be seen on the curve over the range tested (approximately 70 to 1 dynamic range) the change in system delay is bounded by 225 picoseconds. Since electrically generated start and stop pulses are used, the effects of the optical start and stop detectors are not included in this calibration technique.

A second calibration used an optical pulse source. This has the advantage of testing the whole system by exercising the optical detectors as well as the other electronic components in the receiver. The pulse source used in this test was a Power Technology Inc. diode laser pulser Model #IL4C10. Averaging 1000 or 10000 time interval measurements at each pulse amplitude gives the curves shown

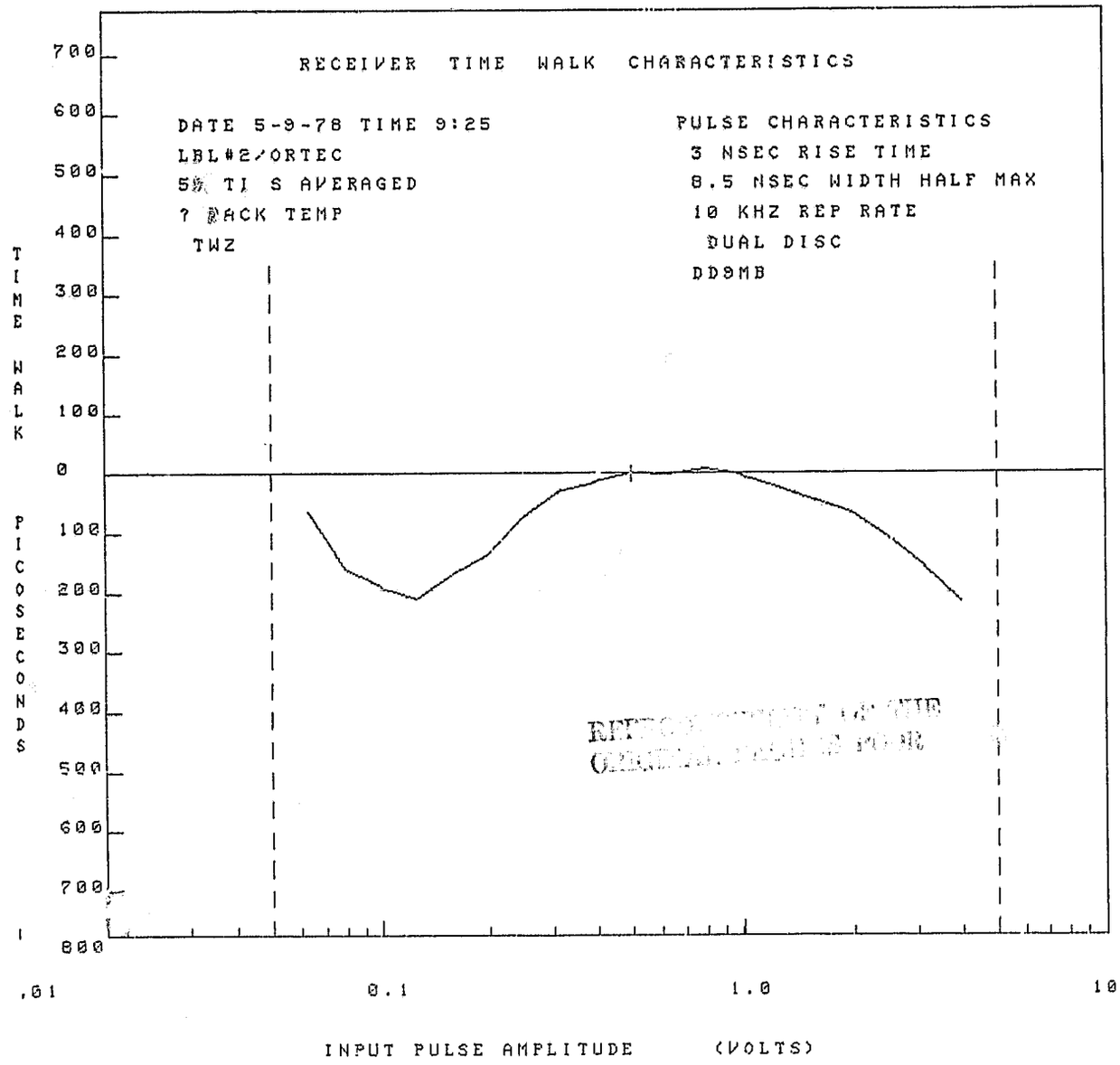

Figure 13. Dependence of the Phase I Receiver Time Walk on the Amplitude of an Electrically Generated Stop Pulse

in Fig. 14. The pre-calibration curve was taken after the receiver configuration was finalized and before any range data was taken. The post-calibration curve was taken after all Phase I range data tests had been completed. The two curves show excellent agreement over the entire amplitude range implying negligible (<50 picoseconds) long term drift in the receiver time walk characteristics. The RMS timing jitter is plotted as a function of pulse amplitude in Figure 14(b). The Hewlett Packard HP5370 time interval unit was used in this calibration run. Repeated calibration curves showed short term repeatability (over several minutes) in the 5 to 10 picosecond range.

This technique was taken one step further when a final laboratory calibration was attempted using the General Photonics laser as the optical pulse source. Poor mean repeatability and large histogram standard deviations on consecutive runs showed that the General Photonics laser could not be used as the pulse source. Repeatability of the mean in identical time interval measurements was typically no better than 200 to 300 picoseconds and as much as 600 picoseconds while standard deviations were in the 500 to 1000 picosecond range.

Pre- and post-absolute time calibration test techniques have not yet been developed for laboratory use. This calibration would require dedicated instrumentation to assure repeatability of system delay measurements days, weeks, or months apart. This absolute timing measurement is in the planning stage. The time walk curves shown in Fig. 14 are relative time measurements only, referenced to the system time delay with a 500 mV pulse amplitude. System time delay at fixed pulse amplitude has been measured over a period of several hours on 2 separate occasions. An afternoon data run of 2 hours 15 minutes shown in Fig. 15(a) reveals approximately a 55 picosecond limit on time drift over that time period. The following morning a 3 hour repeatability run was again made with the results shown in Fig. 15(b). System time drift here was bounded by 40 picoseconds.

Most data taking with the General Photonics laser was no longer than 3 hours in duration and was generally fit into the work day in morning and afternoon sessions. Receiver time drift is apparently responsible for no more than 40 to 55 picoseconds of time drift over a single data taking session.

The effect of received pulse amplitude variation off the water tower may be the major error source degrading overall system accuracy. To test the effect of the receiver under worst case conditions,

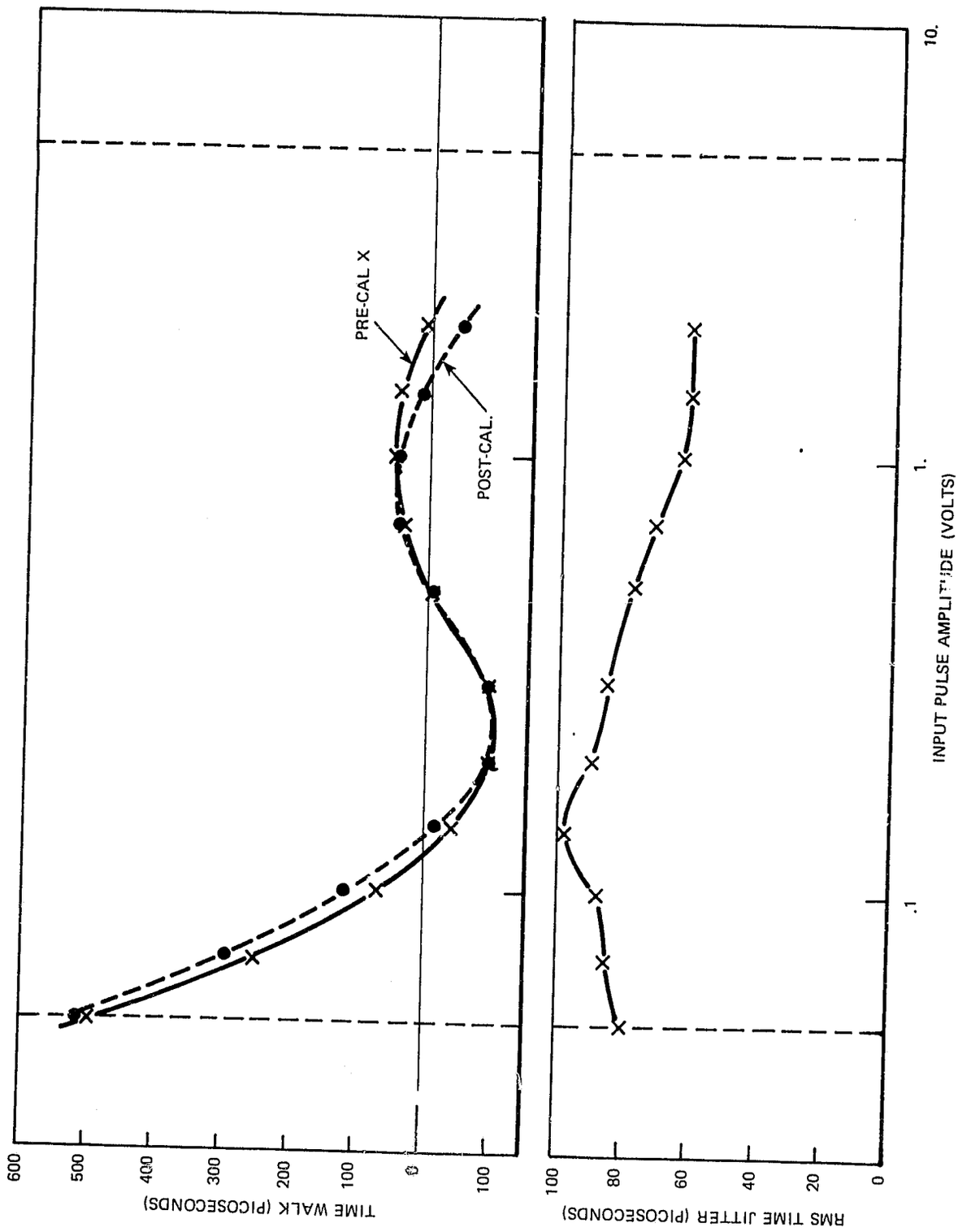

Figure 14. Phase I Receiver Time Walk Characteristics

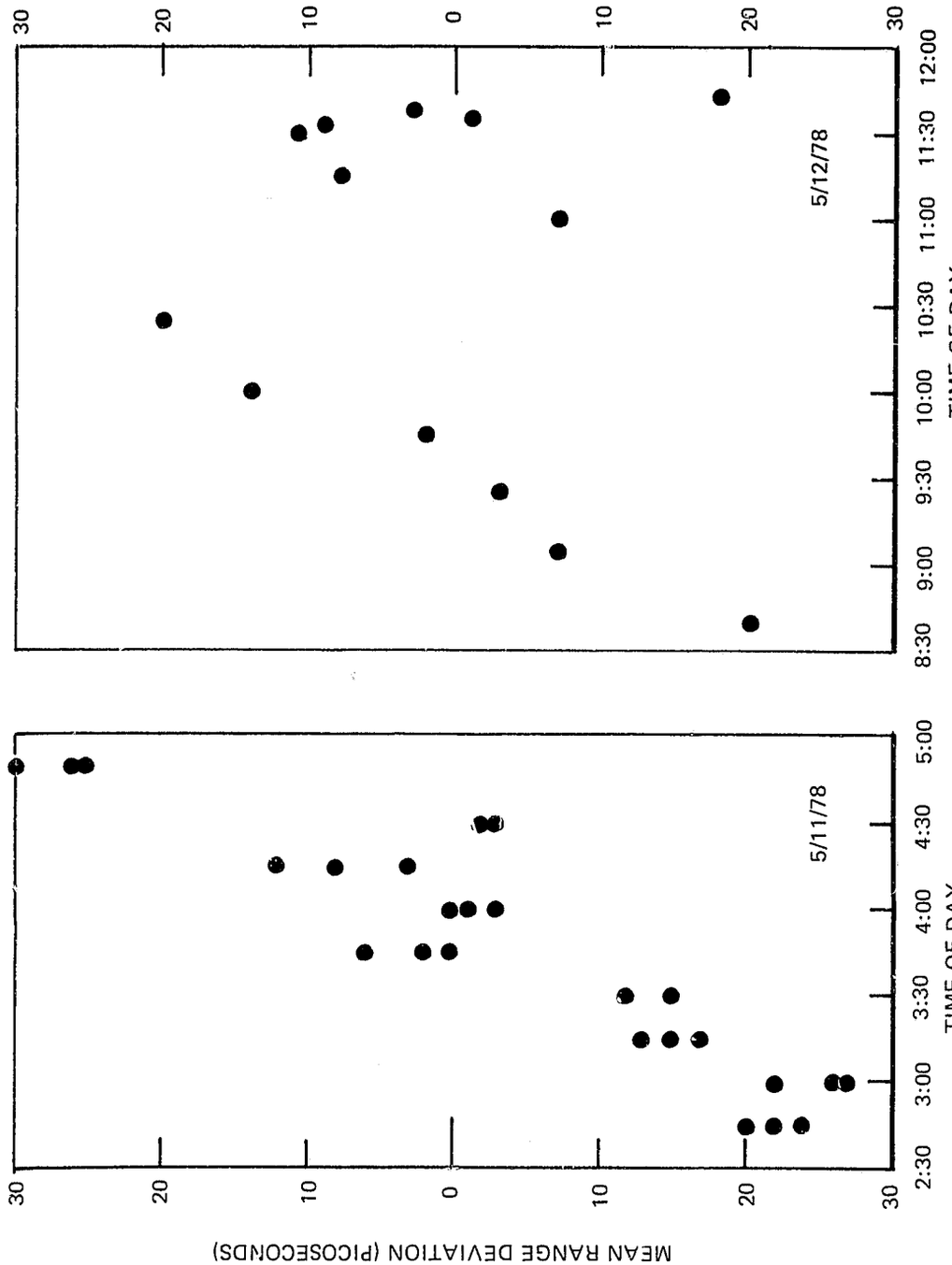

Figure 15. Long-term Repeatability of Phase I Receiver System Delay

the stop pulse amplitude from the diode laser pulse simulator was varied in the lab to give us from 50 mV to 2 volts into the discriminator. Soft saturation of the Sylvania PMT began beyond 2 volts. The time interval measurements were made while the pulse amplitude was varied over the 40 to 1 range using the variable ND attenuator wheel. With a uniform distribution of pulse amplitudes within the 40 to 1 dynamic range, 5000 time interval measurements produced the timing histogram shown in Fig. 16. This worst case situation puts an upper limit on what can be expected from the receiver with a wide variation (40 to 1 range) of signal amplitude. In this worst case condition (uniform amplitude distribution, 40 to 1 dynamic range), the receiver can be responsible for no more than 174 picoseconds of timing jitter. All range data taken off the water tower with the General Photonics laser had pulse amplitude variations of less than 10 to 1 or much less than this worst case (40 to 1). From Fig. 14(b), it can be seen that receiver time jitter is in the range 60 to 100 picoseconds using the HP5370 Time Interval Unit. Time jitter contributed by the HP5360 TIU (used in all water tower range data) has been measured at approximately 109 picoseconds.[3] Considering a dynamic amplitude range of 7 to 1 about the 500 mV level at the stop discriminator input, the ranging system (excluding the laser transmitter) is responsible for no more than 125 to 130 picoseconds RMS time jitter corresponding to about 2 centimeters range jitter. Residual time jitter above this level can be attributed directly to the laser transmitter. To determine the laser's contribution to time jitter in range measurements, an RSS (residual sum of the squares) is computed.

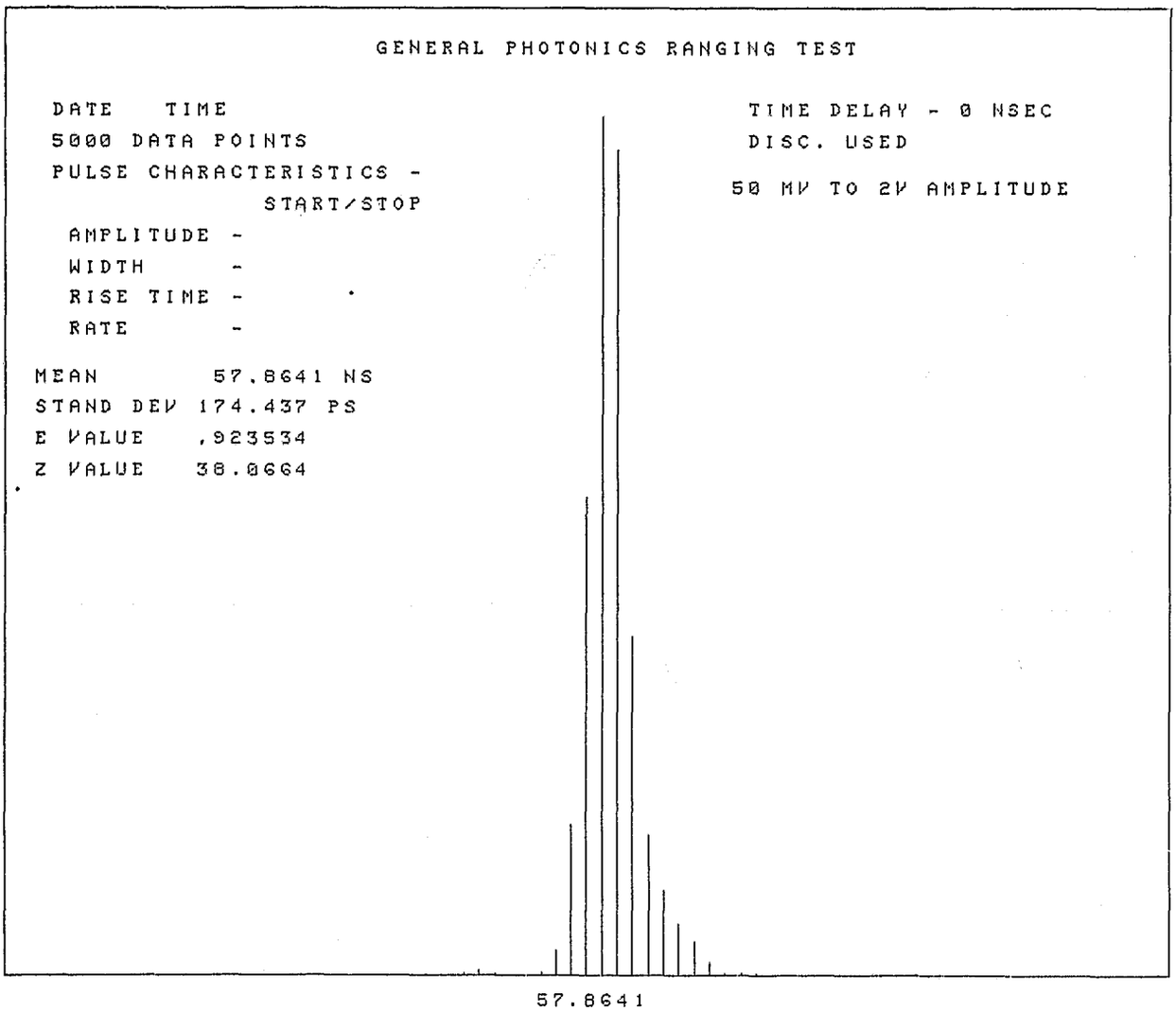

Figure 16. System Delay Histogram for the Phase I Receiver when the Intensity of a Laser Diode Generated Optical Stop Pulse has a Uniform Probability Distribution over a 40 to 1 Dynamic Range. A Total of 5000 Time Interval Measurements Make up the Histogram.

VI. Range Results – Phase I

Using the calibrated receiver described in Section V, range measurements were made to a small one-inch diameter retroreflector placed on a water tower approximately 500 meters from the laser laboratory. The laser beam was directed through the ceiling of the laboratory to a pointing mirror located on the roof of the building. The direction of the pointing mirror can be remotely controlled from the laboratory. Small changes in the azimuthal and elevation axes of the pointing mirror were monitored by pressure-induced voltages on two piezoelectric transducers with a sensitivity of about 0.5 arcseconds/millivolt. In this way, different portions of the laser farfield pattern could be utilized in the range measurement to determine whether or not the multiple transverse mode operation of the General Photonics laser introduces an angularly dependent range error. Using the beam divergence data of Section IV, we compute a beam diameter of about 34 cm at the tower. Thus, the fraction of the total beam cross section intercepted by the retroreflector is

$$F = \left(\frac{2.54}{34}\right)^2 = 6 \times 10^{-3}$$

implying that the retroreflector samples only about 0.6% of the total beam cross-section. As we shall see shortly, the estimate of beam diameter was further verified by the range measurements themselves. The experiment configuration is described in Fig. 12.

When the pointing mirror was aligned for maximum return (on-axis), we observed an approximate 3 to 1 dynamic range in the amplitude of the return signal due to atmospheric fading and/or beam steering effects. Near the outer fringes of the farfield pattern, the amplitude dynamic range was about 8 to 1 and, of course, the absolute returns were much weaker. To eliminate amplitude-dependent time walk characteristics of the receiver as a significant error source, the optical signal into the stop photodetector was attenuated via a variable neutral density filter wheel so that, independent of the particular beam pointing angle, the average input voltage to the stop discriminator was about 500 millivolts. As discussed in Section V, this level is near the center of the low time walk regime of the receiver. This procedure, together with the small dynamic range of the return amplitude, ensures that one nanosecond level differences in the range measurement in the short term will not be

due to the amplitude-dependent receiver time walk. Furthermore, long term thermal drifts in the receiver system delay (or time bias) were shown in the previous section to be less than 60 picoseconds over a three to four hour period.

The effects of atmospheric changes (temperature, pressure, humidity) are insignificant for a roundtrip range of approximately one kilometer as can be seen from the following calculation. The round trip transit time of the pulse is given by

$$t = \frac{c}{2nR}$$

where c is the velocity of light, n is the atmospheric index of refraction, and R is the one-way range to the target. Differentiating the latter expression with respect to n yields

$$\frac{dt}{dn} = -\frac{c}{2\ell}\frac{1}{n^2} = -\frac{t}{n}$$

or

$$dt = -\left(\frac{dn}{n}\right)t$$

Over our range, $t \approx 3145$ nsec. Even with the most extreme atmospheric variation, dn/n will be less than 3×10^{-5} yielding $dt < 100$ psec.[4] This result was verified experimentally by placing an AGA Model 76 He-Ne Laser Geodometer on the roof of the building near the pointing mirror and ranging to the water tower retroreflector. The geodometer data taken over a 24 hour period, is summarized in Table I, and shows a peak-to-peak swing of 8 mm. This eliminates not only atmospheric effects but also long term tower "sway" as a potentially large error source for the laser range measurements to be discussed.

The ranging experiments, using the General Photonics Laser Transmitter as a source, were of two types. The first experiment, a "stability test"[1] was designed to examine the repeatability of the range data mean over a period of several hours. In these tests, the beam pointing angle was fixed such that the retroreflector was always illuminated by the approximate center of the laser far field distribution. The purpose was to study the long term effects of the temporal pulseshape instability on the range measurement. The bandpass filters at the output of the start and stop detectors described

Table I

Results of Geodometer Range Measurements to Water Tower Retroreflector over 22 Hour Period. The Mean Range was 455.811 ± 070027 Meters.

Date	Local Time	Range, X (meters)	$x - \bar{x}$ (mm)
May 11, 1978	4:30 PM	455.808	-3
May 11, 1978	5:30 PM	455.811	0
May 12, 1978	9:30 AM	455.815	+4
May 12, 1978	10:30 AM	455.810	-1
May 12, 1978	11:30 AM	455.807	-4
May 12, 1978	12:30 PM	455.810	-1
May 12, 1978	1:30 PM	455.811	0
May 12, 1978	2:10 PM	455.814	+3

$\bar{x} = 455.811$ meters

$$\sigma^2 = \frac{1}{n-1} \sum_i (x_i - \bar{x})^2 = 7.43 \text{ mm}^2$$

$\sigma = 2.7$ mm

in Section V masked the rapid modulation of the temporal pulse profiles so that smooth waveforms were input to the discriminators during the repeatability tests. The second experiment type is a range map[1] intended to uncover angularly dependent range errors due to multiple transverse mode effects. Since the various transverse modes have different optical losses[5] and effective gains and compete with each other within the Q-switched laser resonator, their pulse buildup times can vary relative to one another. Different transverse modes also have different antenna lobe patterns in the far field[5] of the transmitter. The combination of these two effects can lead to range biases which depend on the position of the retroreflector in the far field antenna pattern of the transmitter laser.

Based on the poor temporal pulseshape stability described in Section II of this report, one would not expect good results from the "stability tests." The expectation is borne out by the experimental data in Figs. 17(a) and 17(b) which were obtained on May 10, 1978, and May 19, 1978

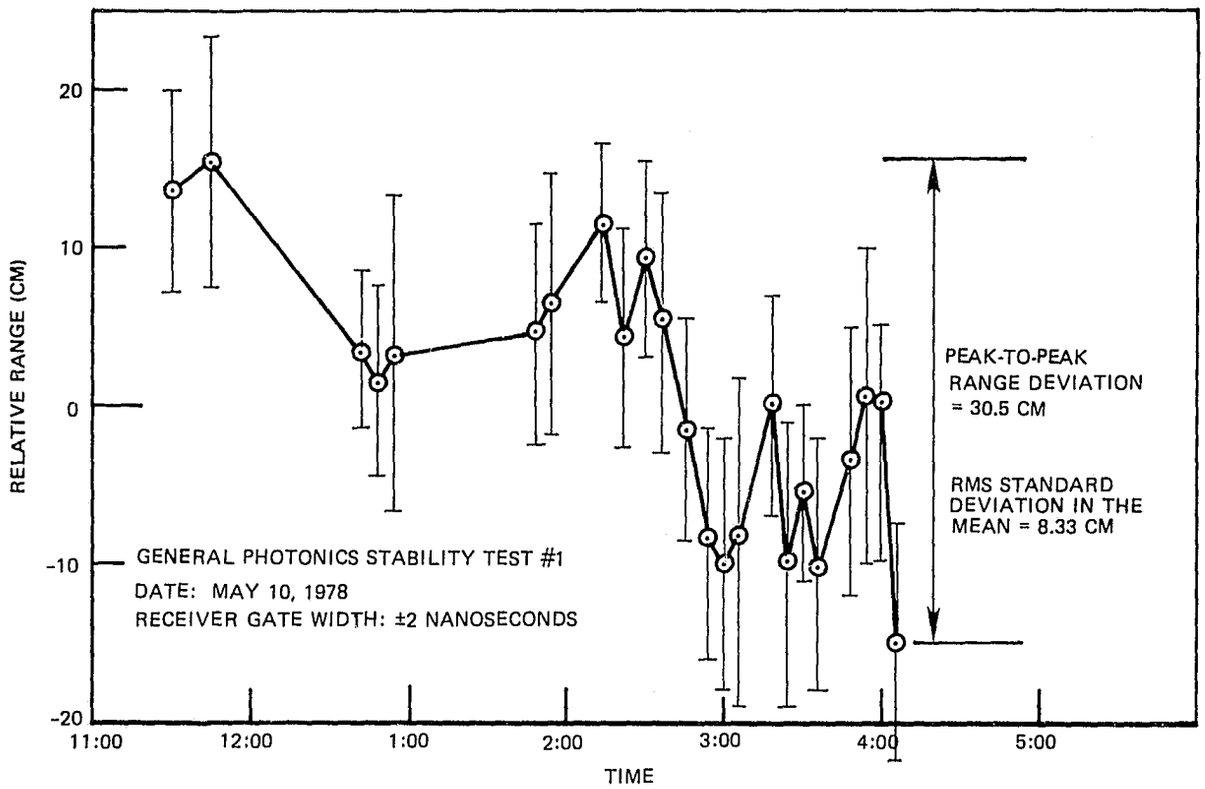

Figure 17(a). Range Stability Test of May 10, 1978. General Photonics Laser (Phase I) and Receiver in Figure 12.

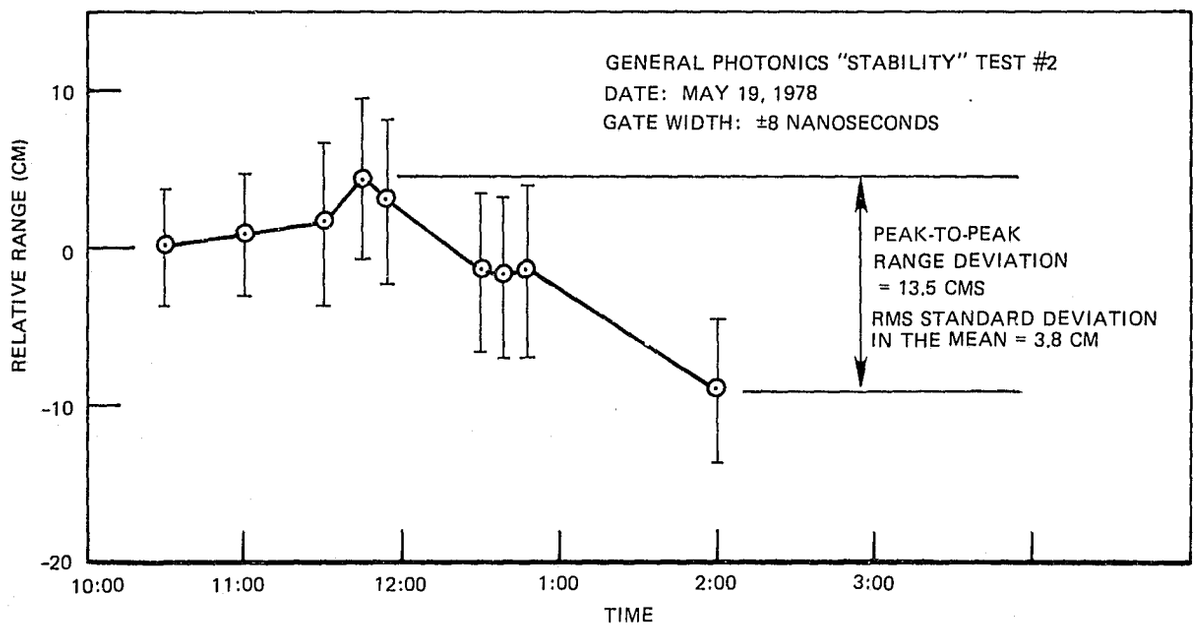

Figure 17(b). Range Stability Test of May 19, 1978. General Photonic Laser (Phase I) and Receiver in Figure 12.

respectively. The individual data points correspond to the means computed from 100 successive ranges to the water tower retroreflector and the error bars indicate the RMS standard deviation (one sigma) of the 100 point data set. For the data of May 10, 1978, an RMS standard deviation in the mean range of 8.33 cms was observed with a peak-to-peak mean range deviation of 30.5 cms. A software generated gate rejected ranges outside a ±2 nanosecond window. On May 19, 1978, the gate was widened to ±8 nanoseconds and an RMS standard deviation in the mean of 3.8 cm was measured with a peak-to-peak deviation of 13.5 cms over a time interval of approximately four hours. On the basis of the receiver calibration tests (time walk, long-term thermal drift) and the geodometer measurements, we are forced to conclude that these large range errors are due to the non-stationary temporal profile of the laser.

The nonstationary characteristics of the laser cloud the interpretation of the far field range map measurements but we present them here for the sake of completeness and to illustrate certain interesting effects. We first outline the procedure which was followed in generating the range map. The pointing mirror was first aligned for maximum signal return. With the mirror fixed at this on-axis position, the average signal level to the discriminator was adjusted to the 500 mV operating point and a large number of ranges (1000) were taken as a precalibration point. Software in the PDP-11 computer then calculated the data mean and standard deviation and plotted the range histogram on the CRT display. The histogram for the 1000 point calibration run taken on May 23, 1978 is shown in Fig. 18 where a mean roundtrip transit time of 3144.69 nsec (includes fixed system bias) and a standard deviation of 541 picoseconds was observed. The latter value corresponds to a ±8.1 cm (one sigma) RMS range error. For this particular run, the 1.06μ energy was 495 mJ. The green energy, however, was only 181 mJ as a result of the modified alignment procedure, described in Section III, which tended to suppress self-modelocking somewhat but did not eliminate it entirely. An earlier map, taken with almost 250 mJ of green energy, gave results similar to those that will be described in detail here.

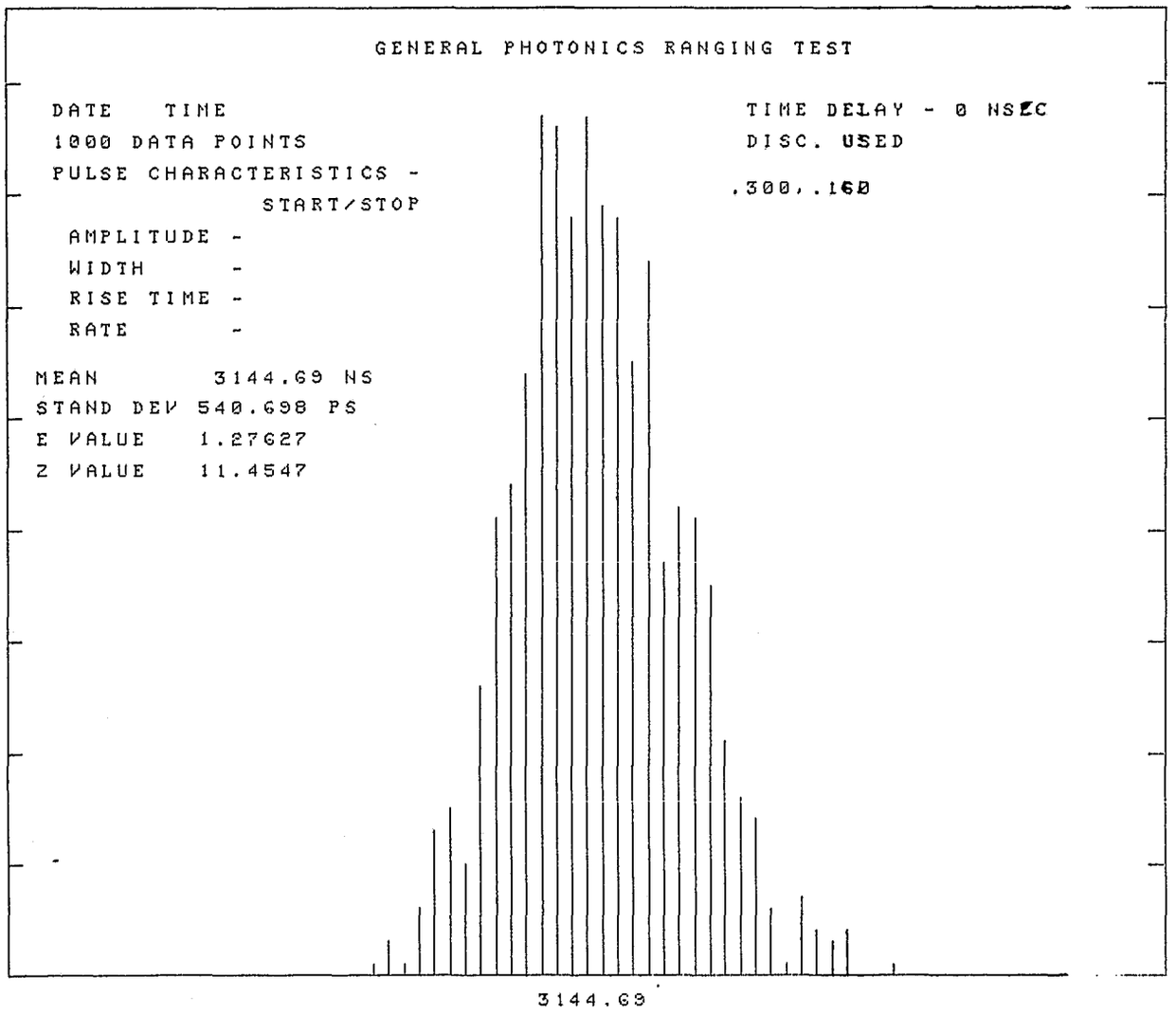

Figure 18. Pre-Calibration Run for Range Map Taken May 23-24, 1978. Beam Direction: "On-axis." Total number of range measurements: 1000 Bin Resolution: 100 picoseconds

After the initial calibration run; the following procedure was used in generating the range map:

1. Change beam direction by a 25 to 30 arcsecond step in one axis
2. Adjust receiver signal level for the center of the low time walk regime (≈500 mV).
3. Take two sets of range measurements of 100 data points each.
4. Subtract the on-axis calibration run mean range from the two local means and express the differences in centimeters of range bias error.
5. Plot the results on graph paper and repeat steps 1 through 4.

In all of our range measurements, the pulse repetition rate was held at 1 pps as in the field operations. In addition, the temporal shape of the return signal was monitored on the Tektronix Model R7912 waveform digitizer.

The range map illustrated in Fig. 19 was taken over a two day period beginning the afternoon of May 23, 1978 and ending the morning of May 24, 1978. The first day was sunny while the second was characterized by moderate fog. The numbered circles and arrows indicate the order in which the data was taken. The twenty grid points marked by "X" were taken on May 23 beginning with the 1000 point precalibration as displayed in Fig. 18. The remaining thirteen points marked by "+" were obtained the following day ending with the 1000 point "on-axis" post-calibration run shown in Fig. 20. The two numbers associated with each grid point correspond to the deviation of the mean range of two successive 100 point data sets from that of the calibration run of the same day. In other words, the mean range for the "on-axis" precalibration run was subtracted from the local "off-axis" means obtained on May 23 while the mean range for the "on-axis" post calibration run was subtracted from the local "off-axis" means obtained on May 24. It should be noted that the mean of the post calibration run differs from that of the precalibration run by 910 picoseconds (or a one-way range difference of 13.6 cm) even though the standard deviation of the post calibration data was only 278 picoseconds (±4.2 cm RMS, one sigma). This is attributed to the nonstationary character of the temporal profile described previously.

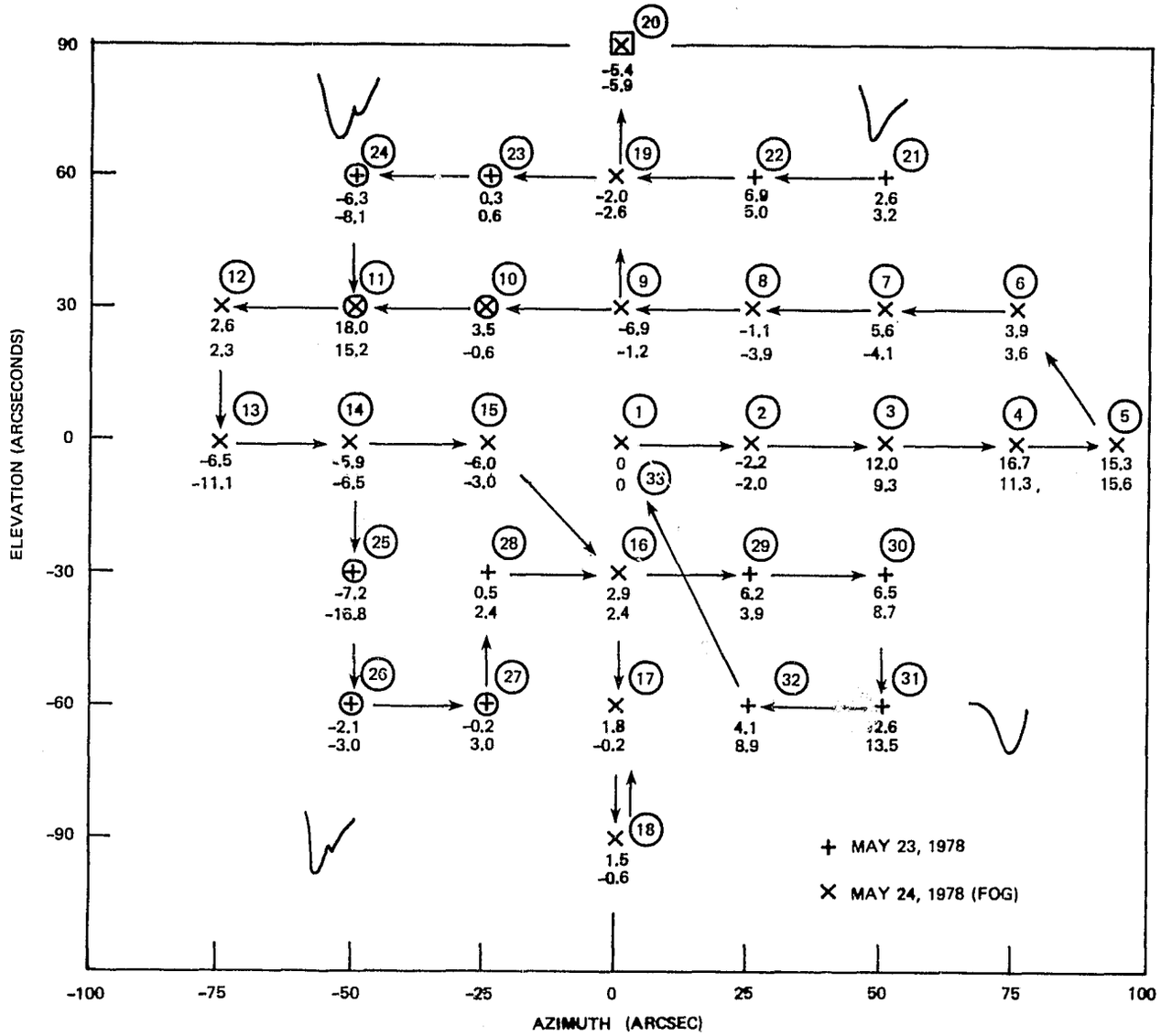

Figure 19. Range Map (in cm) of May 23-24, 1978. General Photonics Laser (Phase I) and Receiver in Figure 12.

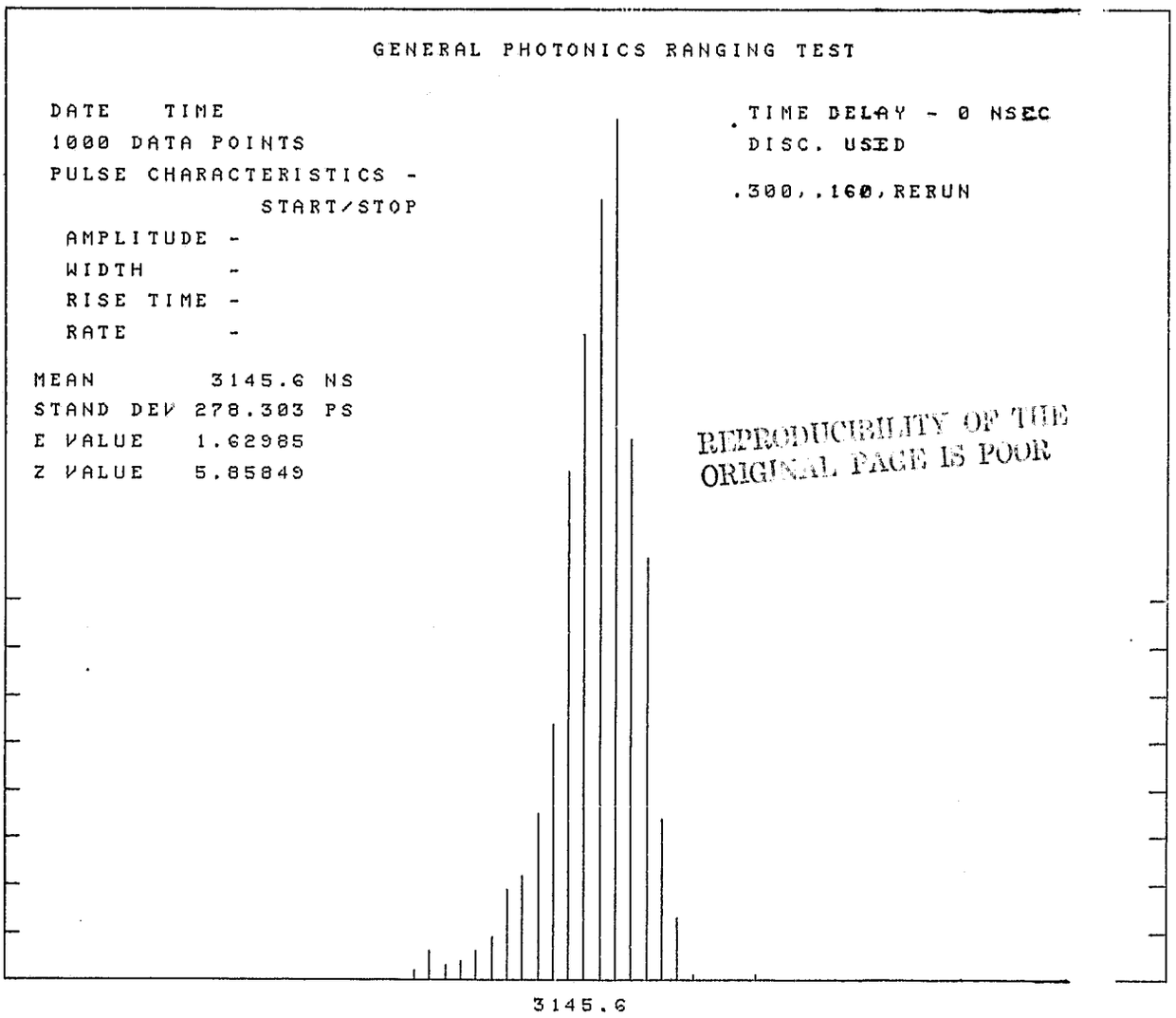

Figure 20. Post-calibration Run for the Range Map taken May 23-24, 1978. Beam Direction: "On-axis." Total Number of Range Measurements: 1000. Bin Resolution: 100 Picoseconds.

The maximum RMS standard deviation for any 100 point data set taken during the range map was 705 picoseconds (±10.6 cm) while the minimum was 257 picoseconds (±3.9 cm). The data histograms for these extreme cases are shown in Figs. 21(a) and (b) respectively. Typical RMS standard deviations for a single far field point were in the range 400 to 600 picoseconds (6.0 to 9.0 cms). It should be stressed, however, that the peak-to-peak variation in the mean range as a function of far field angle was about 25 to 30 cms in each of the two test days and about 35 cms over the full map as can be computed from Fig. 19.

It is also interesting to note that the pulse waveform returning to the receiver from the retroreflector takes on noticeably different shapes as a function of far field angle even when the 200 MHz low pass filter is present between the Sylvania stop detector and the Tektronix R7912 waveform digitizer used to monitor the return waveform. This is indicated by the crude negative-going profiles drawn in Fig. 19 near grid points #21, 24, 26, and 31. For most of the grid points, the filtered return waveform had a steep forward slope and more slowly falling back slope similar to the average output pulse profile in Fig. 5. However, in the region near grid points #24 and #26, a repeatable secondary peak appeared on the back slope of the pulse envelope. For example, at grid point #11 in the upper left-hand quadrant of Fig. 19, the return waveform showed the same strong modulation described previously and a secondary envelope peak as well. Figure 22(a) shows a sample return waveform at grid point #11 as displayed on the Tektronix R7912 with the 200 MHz low pass filter removed. An average waveform over twenty shots, displayed in Fig. 22(b) and taken without the low-pass filter, also suggests a secondary peak in the temporal envelope which broadens the apparent pulse width of the envelope to about 13 nanoseconds (FWHM) in spite of the fact that the width of the outgoing pulse envelope was never observed to be more than about 7 nanoseconds. This is further evidence that the non-uniform summing of different transverse mode contributions in the far-field is contributing to the system ranging error. Finally, near grid point #31 in Fig. 19, the secondary peak was observed to move to the forward slope of the primary peak with the result that the stop pulse appeared to have a slower rise time than the start pulse.

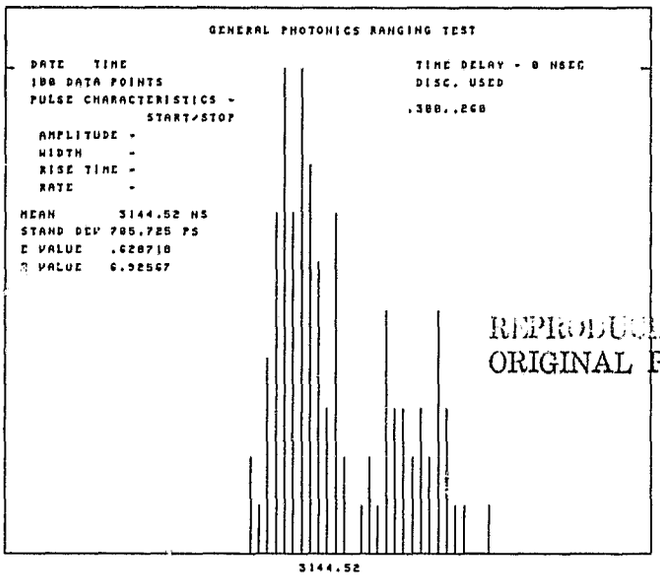

Figure 21(a). Worst Case Range Histogram with Respect to RMS Standard Deviation for Range Map Data Set Summarized in Figure 19. This Histogram was Obtained for Point #19 in Figure 19 and had an RMS Standard Deviation of 705 Picoseconds. Total Number of Range Measurements: 100, Histogram Bin Width: 100 Picoseconds.

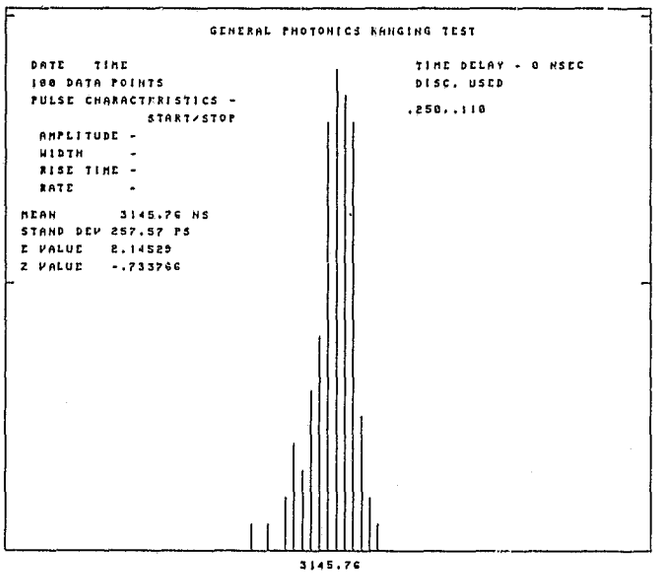

Figure 21(b). Best Case Range Histogram with Respect to RMS Standard Deviation for Range Map Data Set Summarized in Figure 19. This Histogram was Obtained for Point #28 in Figure 19 and had an RMS Standard Deviation of 258 Picoseconds. Total Number of Range Measurements: 100, Histogram Bin Width: 100 Picoseconds.

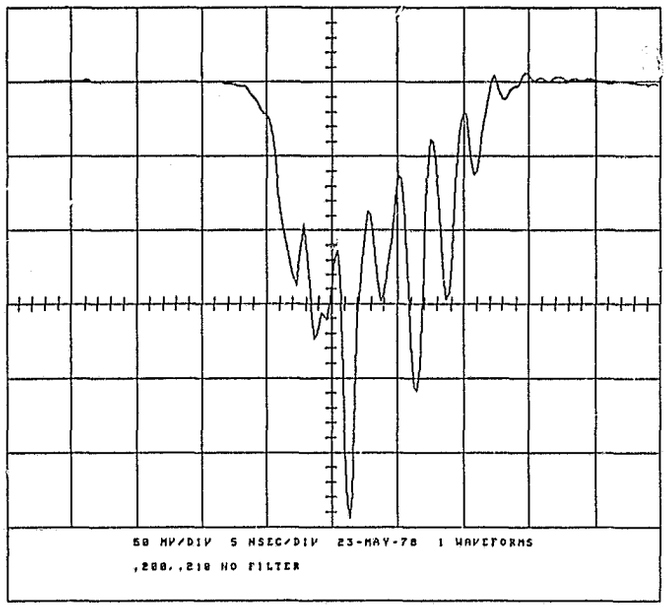

(a)

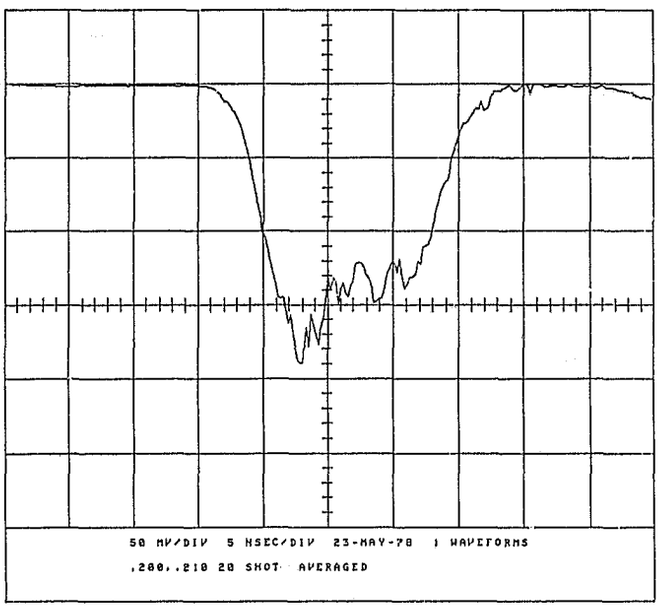

(b)

Figure 22. Sample Return Waveforms as Seen on the Tektronix 7912 Waveform Digitizer with the 200 MHz Lowpass Filter Removed. The Profiles were Obtained at Grid Point #11 in the Range Map of Figure 19. The Single Waveform in Part (a) of the Figure Exhibits Strong Modulation and Suggests a Secondary Peak in the Pulse Envelope. The Average over 20 Waveforms in Part (b) verifies the Secondary Peak which Extends the Effective Pulse Width to about 13 Nanoseconds.

VII. Range Results – Phase II

In the period from June 1978 through September 1978, ongoing laboratory activities required the dismantling of the Phase I ranging system shown in Fig. 12. With the return of the General Photonics laser in late September, an improved ranging system configuration was operational. Using many of the key components of the previous ranging system, the new configuration had several operational advantages and simplified data taking and display.

The new ranging configuration was designed to separate transmit from receive optics. This enabled the receiver optics to be fixed to the target, while transmit optics could steer the beam off axis. Far-field maps taken with the Phase I ranging system required the continual adjusting of a spatial filter in the receiver optical path to correct for walk off. In the Phase II receiver, the periscope/telescope system now remains fixed, while pointing adjustments on the transmitted beam are accomplished with a calibrated pointing mirror in the laboratory.

A simplification in receiver was made possible by combining the separate start/stop channels into a common channel using one detector and one amplifier/attenuator/discriminator chain to the common input on the time interval unit. The single channel system is advantageous since start/stop thermal and amplitude errors track each other. The start chain from the Phase I ranging system was totally eliminated, with the stop chain becoming the start/stop common input. All range data in Phase II was obtained with the receiver configuration shown in Fig. 23. Both start and stop pulse amplitudes were monitored and individually controlled, allowing for amplitude adjustments to minimize receiver time walk effects.

New software was developed on the PDP 11/40 which facilitated data taking, storage and display. BASIC programs loaded from disk into the computer displayed real time range information during beam mappings and repeatability runs. Hard copies of displayed data were available at the end of each data taking set for permanent records.

Optical calibration of the receiver used in the Phase II effort was no longer possible using the common mode input and our laboratory optical pulse simulator. Results of a system calibration,

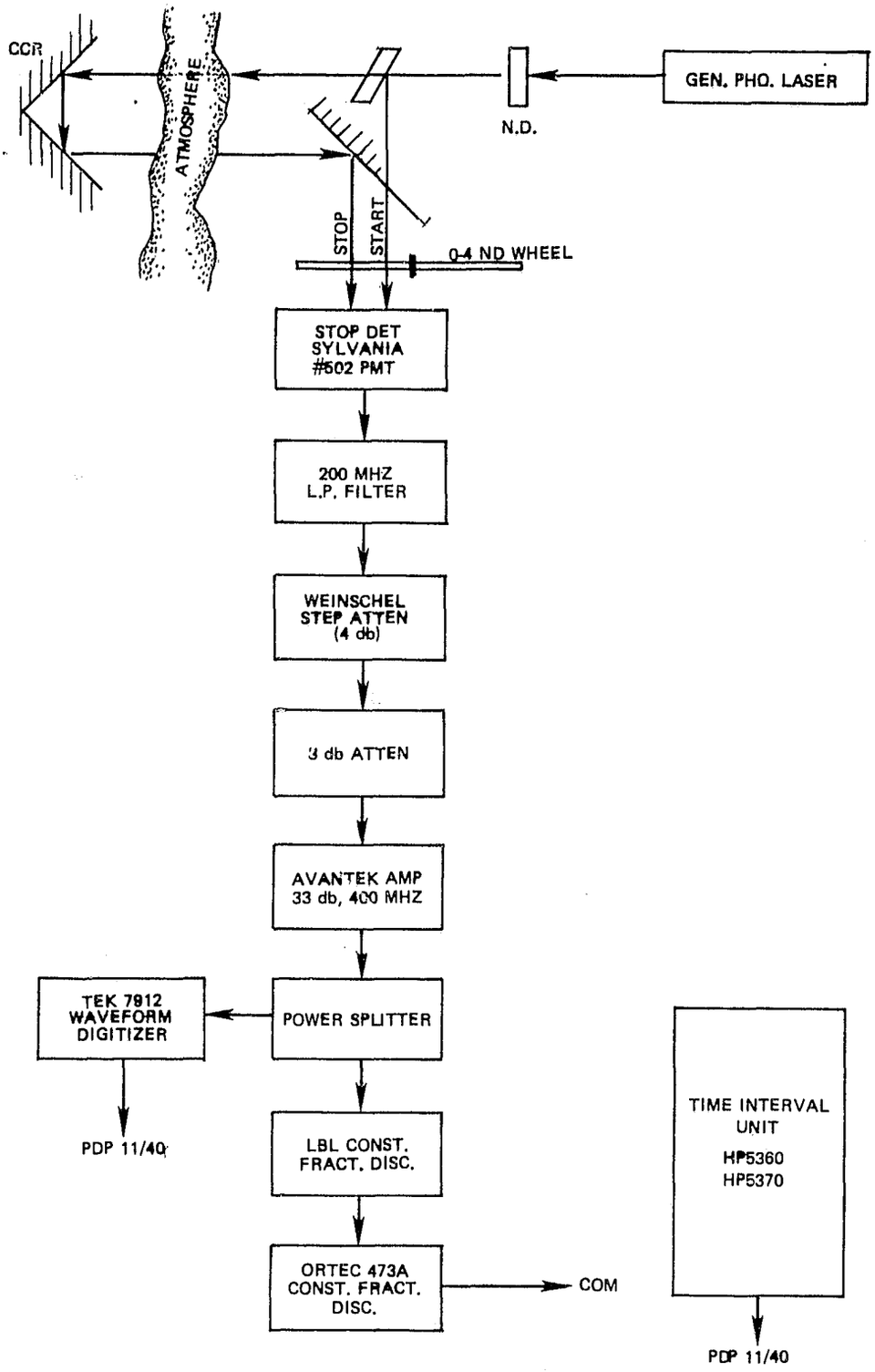

Figure 23. Phase II Receiver Configuration

using an electrically generated start/stop pulse described in Section V, are shown in Fig. 24 using a fixed time delay. Repeatability of measurements on that fixed time interval appears to be at the centimeter level, while RMS jitter is at the 2 centimeter level. The dominant error source in the receiver is discriminator time walk. Figure 25 is a plot of the characteristic time walk curve of the Lawrence Berkeley Lab constant fraction discriminator taken on September 29, 1978. The curve reveals no more than ±150 picoseconds time walk over a dynamic range of 20 to 1. We must conclude, therefore, that the receiver used in Phase II (shown in Fig. 23) was as good as and in many respects better than the dual channel receiver used in Phase I.

Phase II testing of the General Photonics laser began after the laser was returned to Goddard and made operational on September 21, 1978. The only significant difference between the Phase I and Phase II transmitter lasers was a shorter cavity length which resulted in a somewhat shorter Q-switched pulse (4 nanoseconds FWHM in Phase II vs 6 nanoseconds FWHM in Phase I). The shorter cavity length was achieved by removing the highly reflecting mirror in the oscillator cavity and coating one end of the laser rod for maximum reflectivity at 1.06 micrometers. Total energy measurements made on the first day with the Quantronix 506 meter ranged from 300 millijoules to 440 millijoules while the green energy measurement never exceeded 40 millijoules. Because of the poor doubling efficiency, the doubler was removed for inspection. Crystal damage was found on both entry and exit surfaces on the doubler as well as thread damage on the adjusting screws for the doubler itself. Replacements were made the following day and energy measurements were repeated. The total energy was measured at 420 millijoules and the green energy at 150 millijoules. This was typical of the periodic energy measurements made throughout the Phase II testing and was somewhat lower than the Phase I values.

Incoming and outgoing temporal pulse profiles were continuously monitored throughout the testing. Typical returns from the 1 inch retroreflector on the tower are shown in Fig. 26(a) through 26(e). Pulse widths as narrow as 2 nanoseconds were observed but more commonly the values were in the 3 to 5 nanosecond range (FWHM). Full mode locking was still apparent in many pulses with

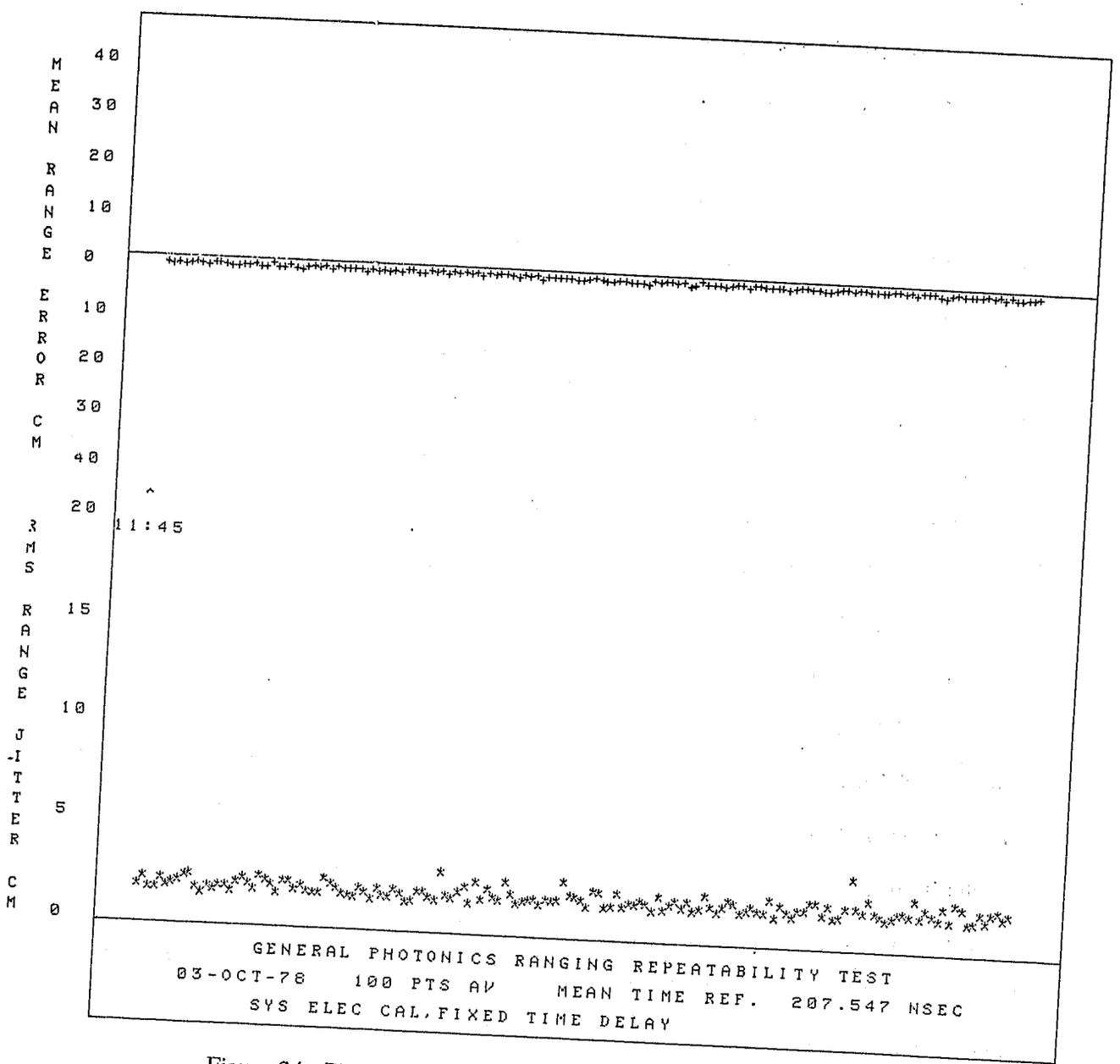

Figure 24. Phase II Receiver Repeatability using an Electrically Generated Start/Stop Pulse and a Fixed Time Delay.

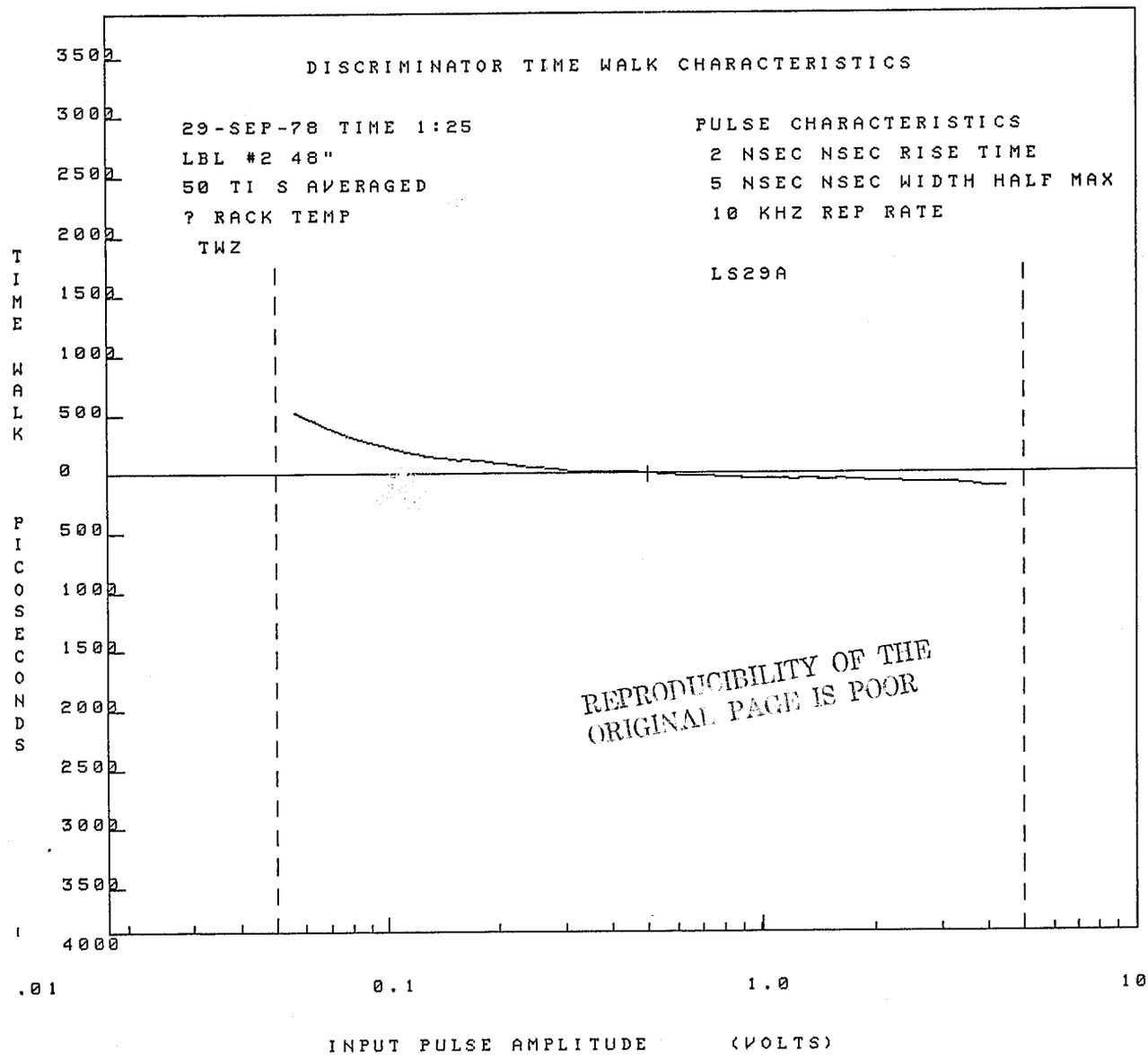

Figure 25. Time Walk Characteristics of the Lawrence Berkeley Lab Constant Fraction Discriminator as a Function of Input Pulse Amplitude.

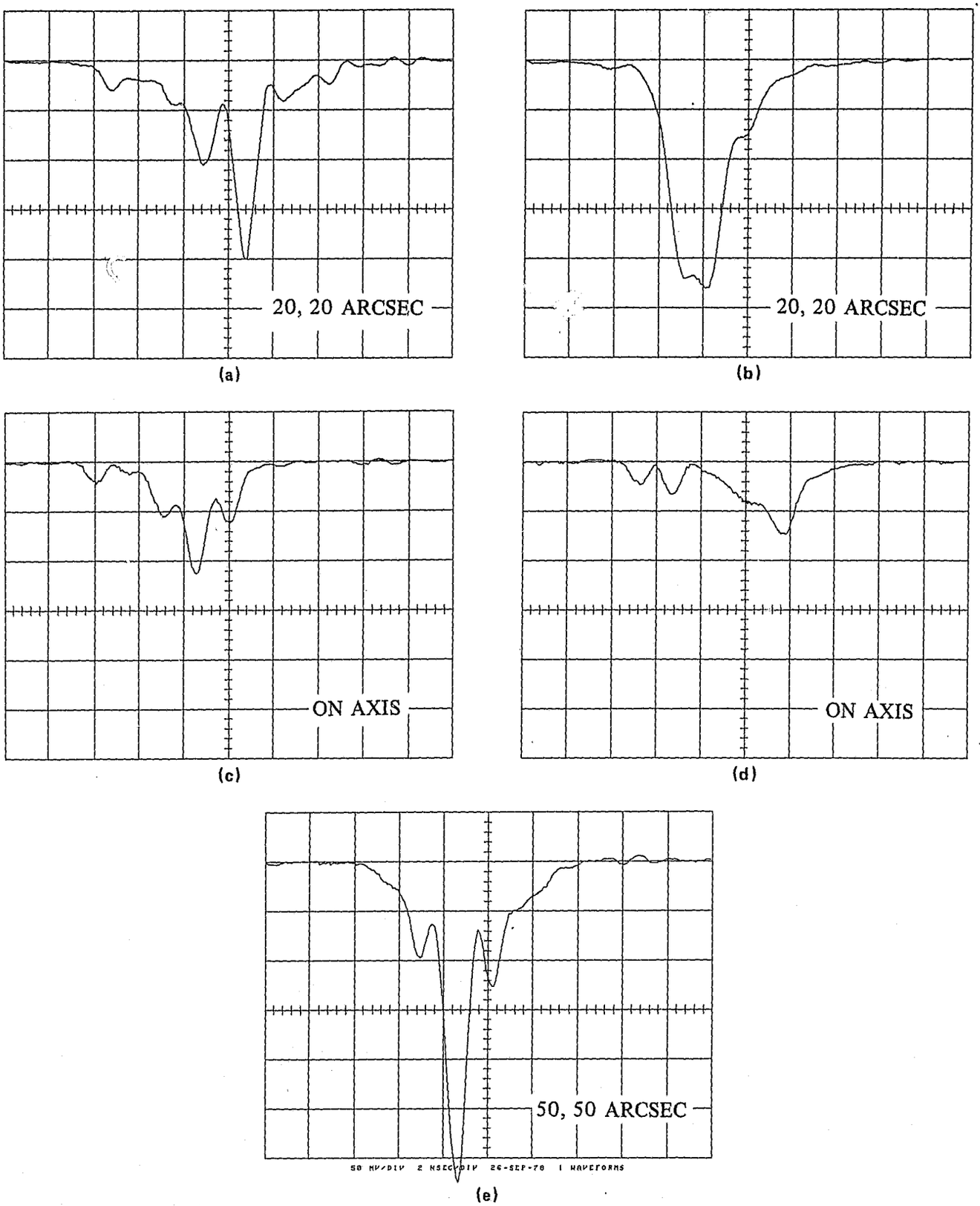

Figure 26. Typical On-Axis and Off-Axis Waveforms Returned by the Retroreflector as Monitored by the Tektronix R7912 Waveform Digitizer with the Low-pass Filter Removed from the Output of the Sylvania Photomultiplier Tube. (50MV/DIV, 2NSEC/DIV).

modulation depths approaching 100%. Several returning waveforms show either long leading or trailing edges and sometimes both while others show multiple peaks separated by approximately 2 nanoseconds. These pulse waveforms are representative of typical on and off axis returns from a retroreflector in the far field. The output of the Sylvania 502 photomultiplier was displayed directly on the Tektronics R7912 waveform digitizer to capture these return waveforms. In short, the temporal profiles observed during Phase II were similar to those observed during Phase I except for the pulse envelope width (FWHM) which was shorter by about two nanoseconds.

Repeatability data taken on-axis on October 11, 1978 with the General Photonics laser is shown in Fig. 27. Both mean range error and RMS range jitter are displayed as a function of the time of day. The mean range error is measured with respect to a mean established by the first (or precalibration) run. The RMS range jitter is the one sigma standard deviation of each 100 time interval measurement set. Each data point displayed in Fig. 27 is spaced approximately to the time of day the data was taken. The vertical scale for mean range error is 10 cm/div. while, for RMS range jitter, it is 5 cm/div. All repeatability data was taken with a ±8 nsec software generated gate. This test, spanning 6 hours, typifies turning the laser on for 15 minutes every half hour throughout the day and recording the on-axis mean range error and RMS jitter. The ranging residuals remained good throughout the test (3-5 centimeters) but the mean range bias error drifted continuously while the laser was operating. Even though the first data point in each 15 minute ranging session is repeatable within about 3 centimeters, the total drift in the system bias over the following 15 minutes of continuous laser operation (10 data sets of 100 points each at 1 pps) has been observed to be as large as 8 cms. Drift in the system bias in Fig. 27 was always in the same direction, with drift rates varying up to .6 cm/minute.

Repeatability data taken with a 5 pps repetition rate is shown in Figs. 28(a) and (b). Again the RMS range jitter for each 100 point data set is on the order of 3 to 6 cms. The system bias, however, was observed to drift in opposite directions on two consecutive days of testing (October 2 and 3, 1978). At 5 pps, the on-axis drift rate was often considerable with the system bias changing by about 25 cms during a 40 minute period on October 2. The rather long time scale of the drift suggests that thermal effects within the laser resonator may be responsible for poor repeatability in the mean range.

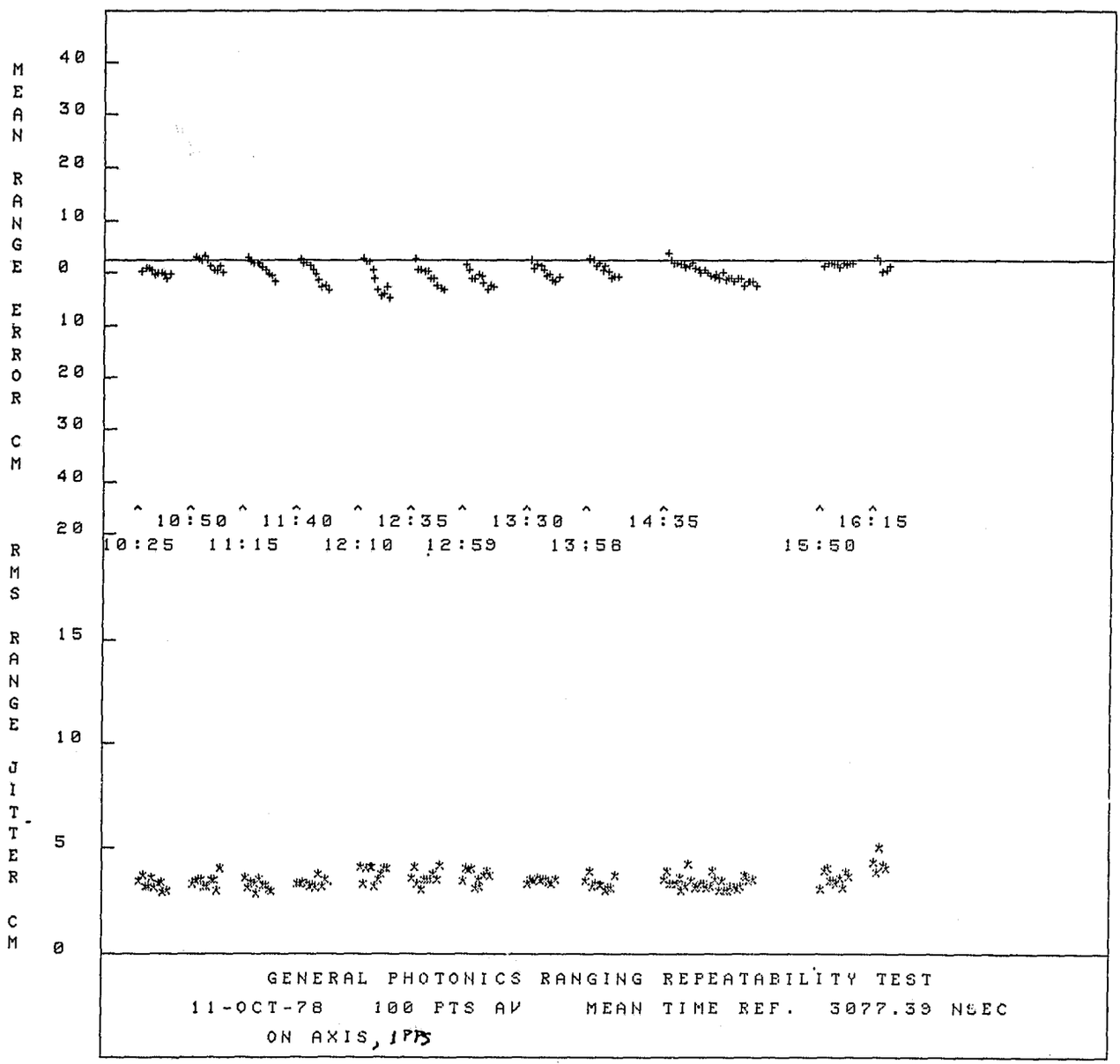

Figure 27. Phase II Repeatability Test with the General Photonics Laser Turned on for 15 Minutes within Each Half-Hour Interval.

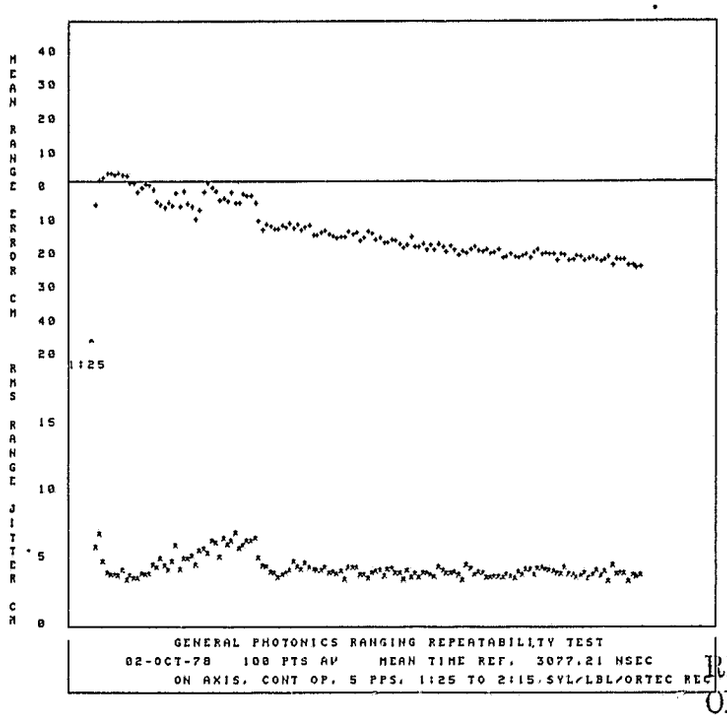

(a)

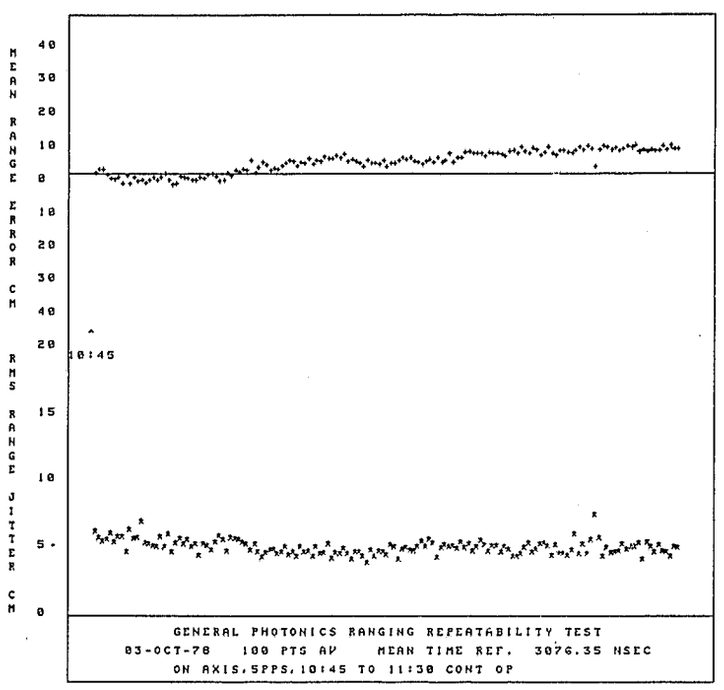

(b)

Figure 28. Phase II Repeatability Tests of the General Photonics Laser for Continuous Operation at 5 pps over: (a) a 50 Minute Interval on October 2, 1978 and (b) a 45 Minute Interval on October 3, 1978.

Repeatability tests performed with off-axis illumination of the retroreflector at 5 pps often showed a cyclic behavior of the mean range with time.

Using the procedures outlined in Section VI, a range map was generated on October 6, 1978 and is shown in Fig. 29. The X and Y axes are in seconds of arc, measured from on-axis (o,o). Two consecutive 100 data point runs were made at each map location, given by the '+'. The first number displayed is the mean value in centimeters referenced to the on-axis value, while the second number is the RMS jitter (also in centimeters) at that map location for the 100 data point set. On-axis (reference) calibration and post calibration are recorded at the top of the page. This data, taken at 1 pps, shows a mean range deviation (peak-to-peak) of 18.2 centimeters, and RMS jitters from 2.4 centimeters to 6.1 centimeters. The energy density at the outer perimeter of the range map is approximately 10% of the peak energy density at the center of the transmitter far field profile with the 4.2 power collimator removed. As stated previously, the stop pulse amplitude was maintained at a constant average level throughout the map through the use of a variable optical attenuator wheel.

Maps taken at laser repetition rates of 5 pps have shown a much greater peak-to-peak mean range deviation than 1 pps maps. One 5 pps map is shown in Fig. 30. The peak-to-peak variation in the mean range of this map is 76 centimeters, while the RMS standard deviations for individual 100 point data sets range from 3 to 12 centimeters. The energy density at the outer perimeter of this map is about 0.1% of the peak energy density on-axis.

The 5 pps data presented here is not intended to represent the performance of the General Photonics Laser in the field where it is operated at 1 pps. However, the 5 pps repetition rate allowed range data to be taken at a correspondingly higher rate during the limited period that the General Photonics was available for testing. The 5 pps data is included in this report only to show that the ranging performance of the General Photonics laser degrades considerably at the higher repetition rate.

Upon completion of the Phase II testing an attempt was made to limit operation of the oscillator to the TEM_{oo} transverse mode. To accomplish this, the mode volume in the rod was reduced by limiting the aperture size within the oscillator. The 3.5 millimeter diameter stop built into the

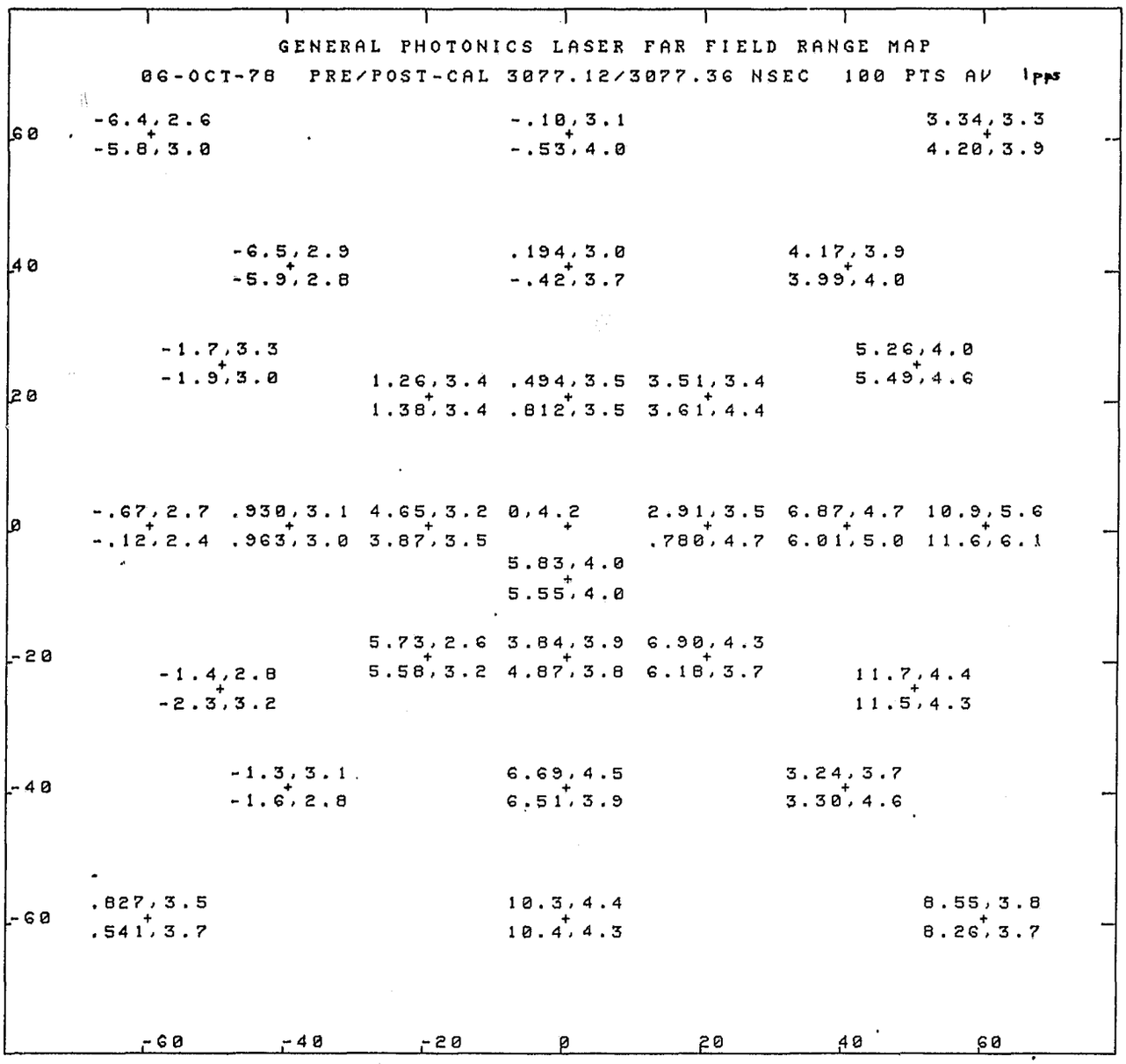

Figure 29. Range Map of the Phase II General Photonics Laser Operated Continuously at a Repetition Rate of 1 pps on Oct. 6, 1978. Peak-to-peak Variation in the Mean Range was 18.2 cms with a One Sigma RMS Standard Deviation in the Mean of 4.5 cms Assuming Uniform Weighting of All Field Angles.

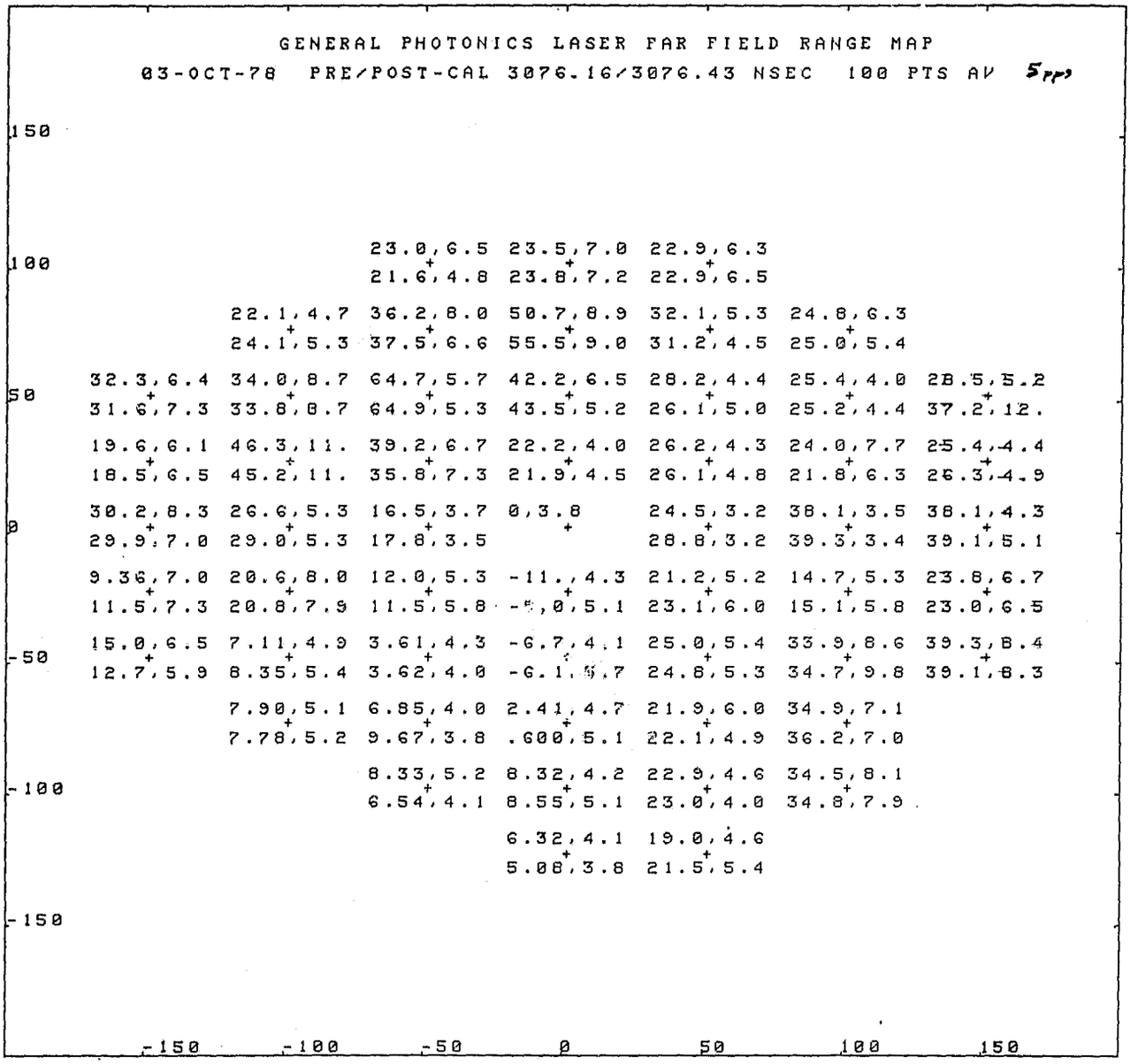

Figure 30. Range map of the Phase II General Photonics Laser Operated Continuously at a Repetition Rate of 5 pps on Oct. 3, 1978. Peak-to-peak Variation in the Mean Range was 75 cms with a One-sigma RMS Standard Deviation in the Mean of 13.5 cms Assuming Uniform Weighting of All Field Angles.

General Photonics laser oscillator was removed and replaced with a mode-limiting aperture having a 0.6 millimeter diameter. While the small aperture produced a clean circular spot, it also appeared to force the laser into a modelocked condition on virtually every pulse. The mode locked pulse train is evident in Fig. 31(a) (an outgoing start pulse) and Fig. 31(b) (a return from a retro-reflector in the far field). The pulse width of the envelope is 8 to 9 nanoseconds (FWHM) with a 6 nanosecond rise time (10% - 90%). The symmetry and slower risetime of the pulse envelope, as recorded on the R7912 Waveform Digitizer, was a result of the low oscillator output energy which no longer saturated the double pass amplifier. With a 300 MHz filter following the photodetector, a smooth profile was observed as in Fig. 31(c) Range residuals, however, were 10 cms on axis at best in spite of the low band-pass filter. RMS range jitter off axis increased to 15 to 27 centimeters with mean range variations of almost 43 centimeters peak-to-peak as in the range map of Figure 32. Based on these results, it is clear that TEM_{oo} mode operation will not improve the ranging performance unless longitudinal mode competition is also suppressed.

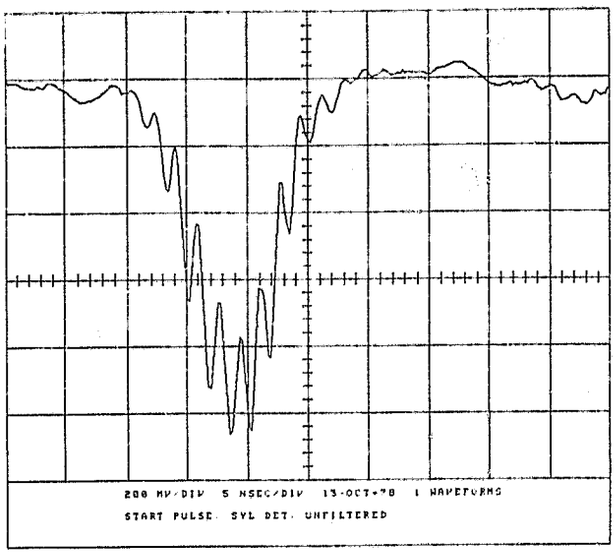

(a)

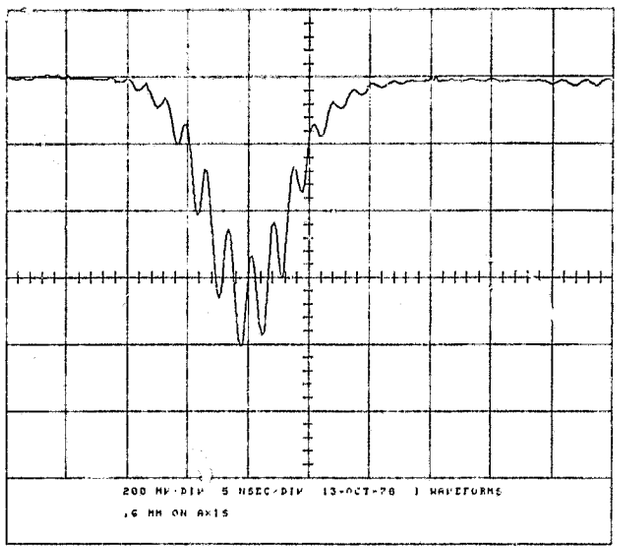

(b)

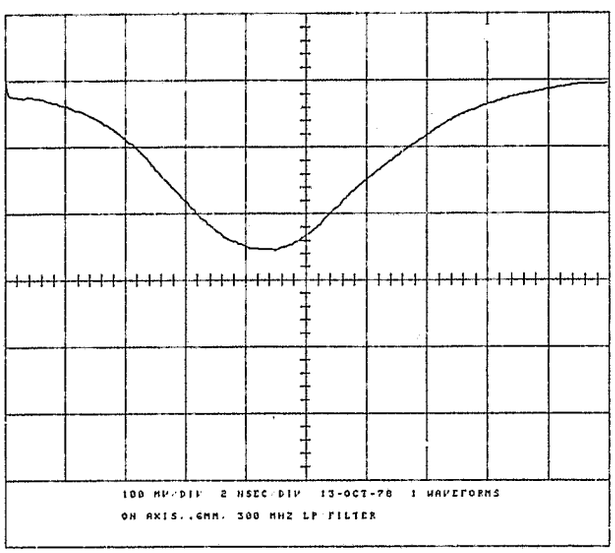

(c)

Figure 31. Pulse Profiles from the General Photonics Laser after a 0.6 mm Diameter Mode-limiting Aperture was Installed in the Oscillator to Suppress High-order Transverse Modes: (a) a typical start pulse; (b) a typical stop pulse from the tower; and (c) a typical stop pulse as seen through the low bandpass filter in the Phase II receiver.

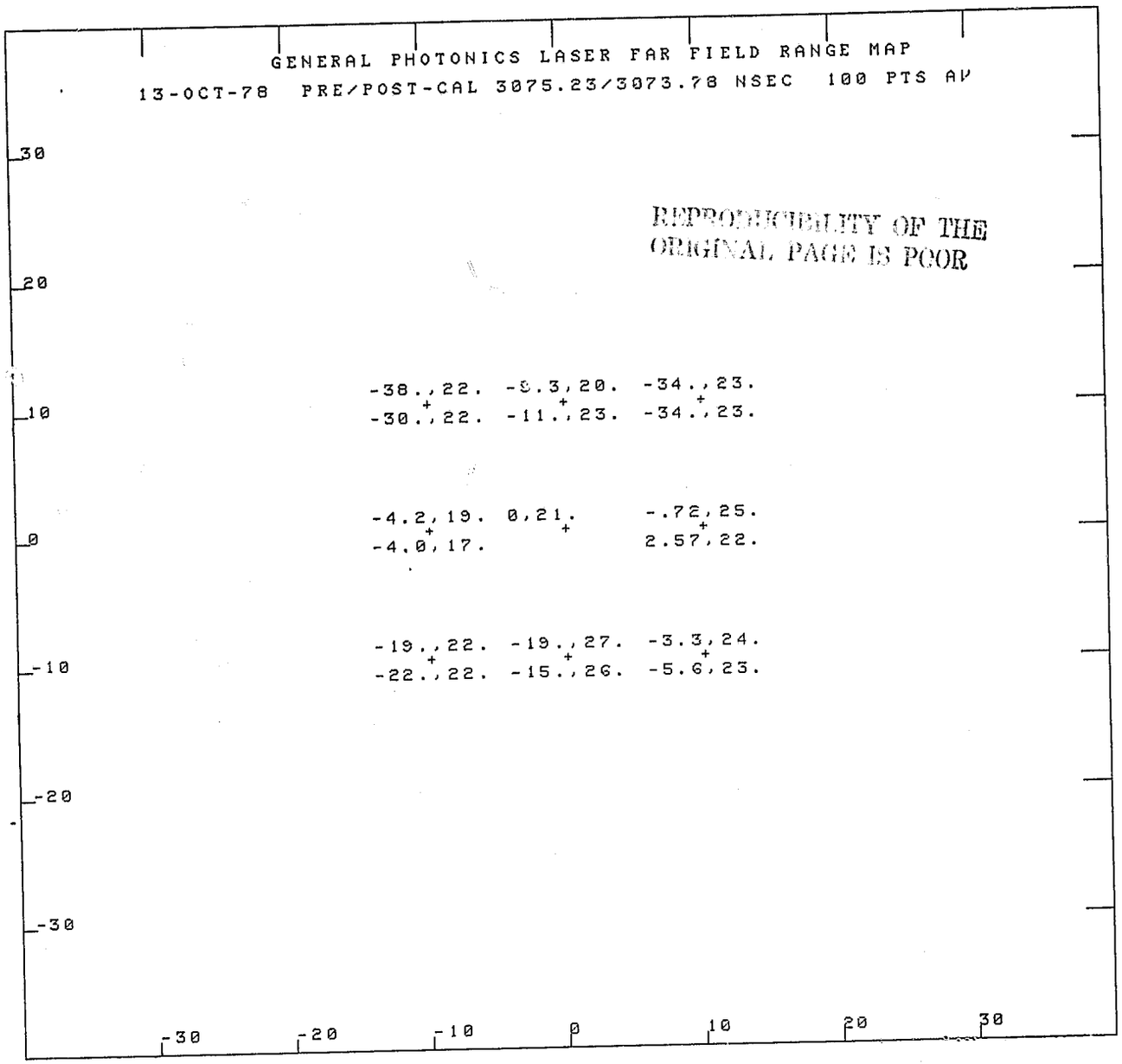

Figure 32. Far Field Range Map Obtained when a 0.4 mm Diameter Aperture was Inserted into the Phase II General Photonics Oscillator to Limit Operation to the TEM_{oo} Mode. The Laser Modelocked Strongly on Each and Every Pulse and the RMS Standard Deviations, Given by the Second Number at Each Grid Point, were Typically in the 20 cm Range.

VIII. Phase III Range Results with a Cavity-Dumped Oscillator

The cavity-dumped version of the General Photonics laser was delivered to Goddard and testing began on Nov. 29, 1978. Initial measurements of the temporal profile indicated a rather slow rise-time on the pulse and a pulsewidth corresponding to several roundtrip transit times of the cavity. This suggested that the electro-optic cavity dump switch was not operating properly. Measurement of the voltage waveform with a high speed (3 nsec rise), high voltage oscilloscope probe indicated a switch risetime in excess of 10 nanoseconds. Furthermore, optical damage on the oscillator rod was discovered. A new oscillator was installed and testing was reinitiated on December 6, 1978.

The average pulse waveform (40 shots) of the new oscillator is displayed in Fig. 33(a). The pulse-width was about 3.6 nsec between the half-maximum points and about 10 nsec between the 10% intensity points. Individual pulses still displayed a fair amount of modulation as can be seen from Fig. 33(b). The latter waveforms were obtained after a General Photonics technician completed his adjustment of the optical alignment and cavity dump timing. The rather long pulses again indicated a rather slow cavity dump switch, but it was decided to obtain some range measurements before further modifications were made.

It should be mentioned that the Phase II receiver was not available for these initial tests. A somewhat different 5 nanosecond receiver, built for the Spaceborne Geodynamic Ranging System (SGRS), was available, however. The receiver, illustrated in block diagram form in Fig. 34, utilizes a matched filter (tapped delay line) and peak detector instead of constant fraction discriminators. The SGRS receiver, to be described in detail elsewhere,[8] is an implementation of a maximum likelihood receiver which attempts to take into account, in a near optimum way, the Poisson statistics associated with photoelectron generation in the detector. Previous calibrations of the receiver[8] have indicated a performance which is within 3 dB of the theoretical limit. Thus, the SGRS receiver time walk characteristics are as good or better than that of the Phase II receiver.

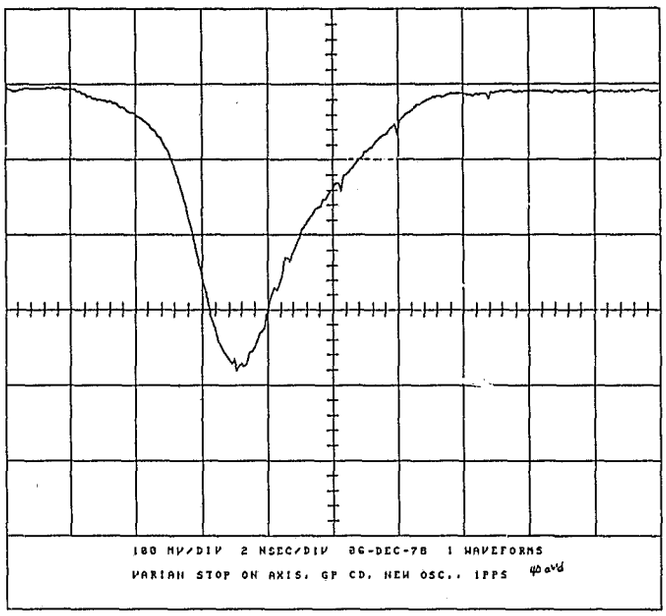

Figure 33(a). Average Temporal Waveform of the General Photonics Laser using the Contractor Supplied Cavity Dump Switch. Forty Individual Waveforms were Averaged to Obtain the Profile. The Pulsewidth is 3.6 Nanoseconds between the Half-maximum points and 8.8 Nanoseconds between the 10% of Full Intensity Points.

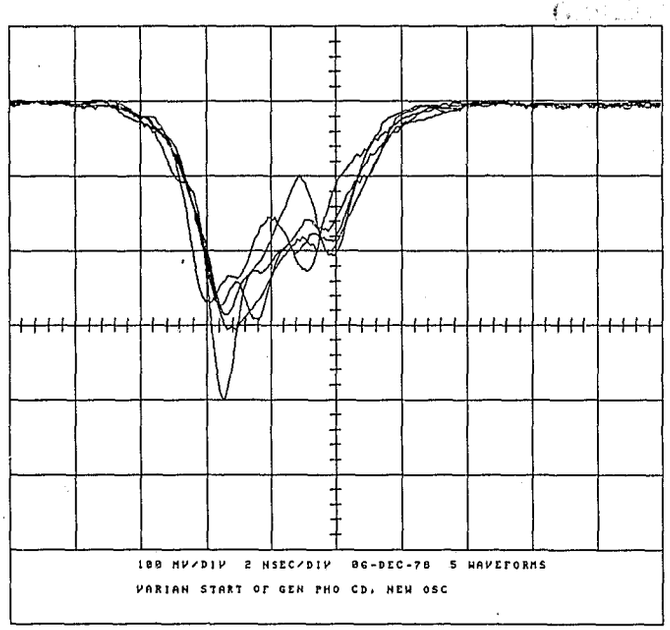

Figure 33(b). Several Individual Pulse Profiles from the General Photonics Laser using the Contractor-supplied Switch. Significant Modulation is Still Evident.

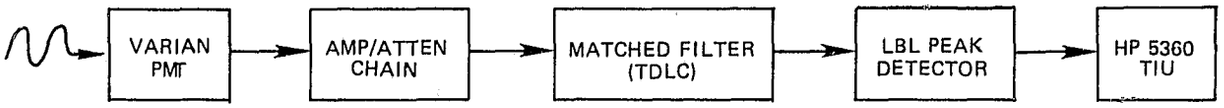

Figure 34. SGRS Receiver

The quality of the ranging results were mixed. Figure 35 displays the results of a repeatability test obtained with the Phase II cavity-dumped General Photonics Laser and SGRS receiver. The data shows a 1.5 cm peak-to-peak variation in the mean range over a 90 minute interval. Each data point in Figure 35 represents the mean of 100 single range measurements at a repetition rate of 1 pps. This data represents a significant improvement over the repeatability data obtained during the Phase I and Phase II tests. The RMS range jitter recorded during this test was stable at about 3 cms (one sigma).

The results of a far-field map taken the same day are shown in Figure 36. The peak-to-peak variation in the mean range was 17.9 cms and the RMS standard deviation in the mean was 5.4 cms with all pointing angles weighted equally. When operated in the field, the laser output is transmitted through a 4.2 power collimator. Therefore, the data in Figure 34 is representative of the expected performance over a 36 arcsecond radius cone in the final field system.

Clearly the results of the Phase III stability test were quite good compared to the Phase I and Phase II tests. The range map, on the other hand, was not much better than before. It was therefore decided to replace the contractor-supplied switch with an inhouse design[9] which utilized high speed (<1 nsec) krytron switches. The resulting waveforms, illustrated in Fig. 37(a), indicate a subnanosecond (10% to 90%) risetime, a FWHM pulsewidth of 1.5 nsec, and a baseline pulsewidth (between 10% points) of only 3 nsec. Return waveforms from the tower possessed similar properties both on and 100 arcseconds off axis as in Figures 37(b) and 37(c). It was found that triggering the cavity dump switch well beyond the peak of the internal Q-switch buildup gave the steepest forward slope and the best range results. To insure that we encountered no optical damage problems with the short pulse width, the lamp voltage to the oscillator was set at its lowest value. The combined effects of reduced pump energy and switching beyond the Q-switch peak resulted in a greatly reduced oscillator output.

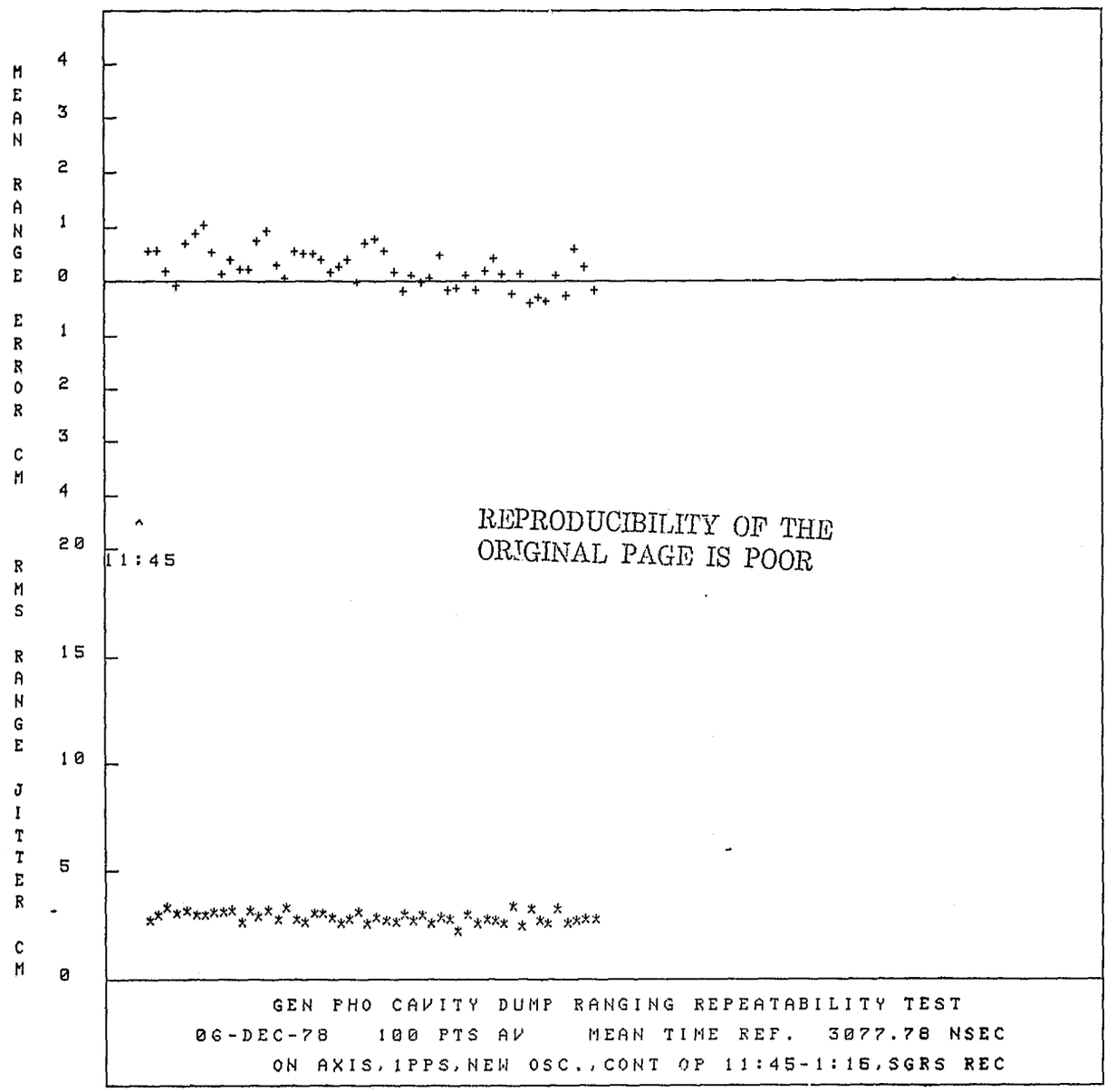

Figure 35. Range Repeatability Test of the Phase III Cavity Dumped General Photonics Laser Obtained on December 6, 1978 with the SGRS Receiver. The Peak-to-peak Error in the Mean Range was 1.5 cms over a 90 Minute Interval. Each Mean Range was Computed from a Data Set of 100 Range Measurements taken at a Repetition Rate of 1 pps. The Standard Deviation for Each Data Set is Typically 3 cms.

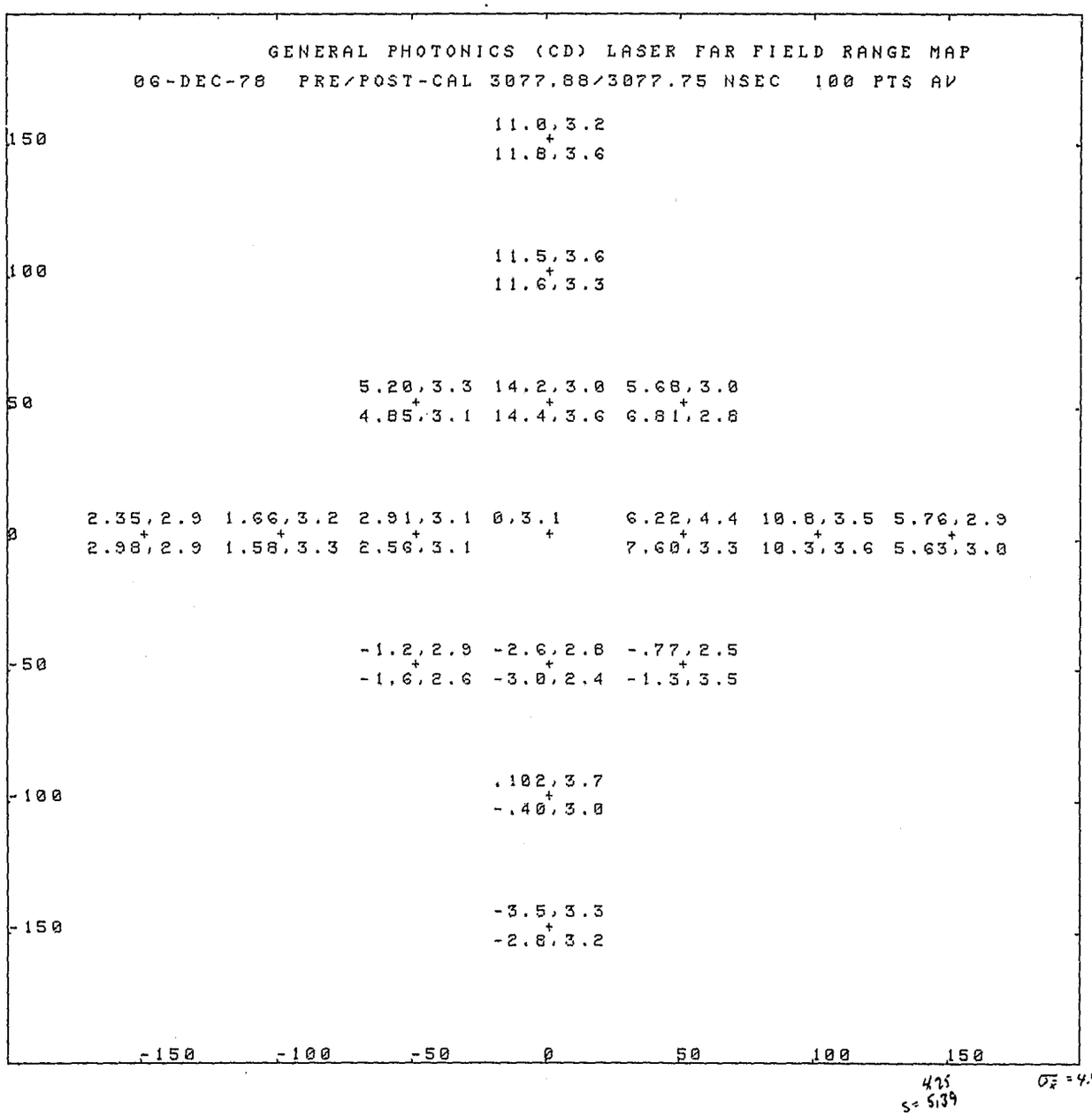

Figure 36. A Preliminary Range Map using the Phase III Cavity-dumped General Photonics Laser and SGRS Receiver.

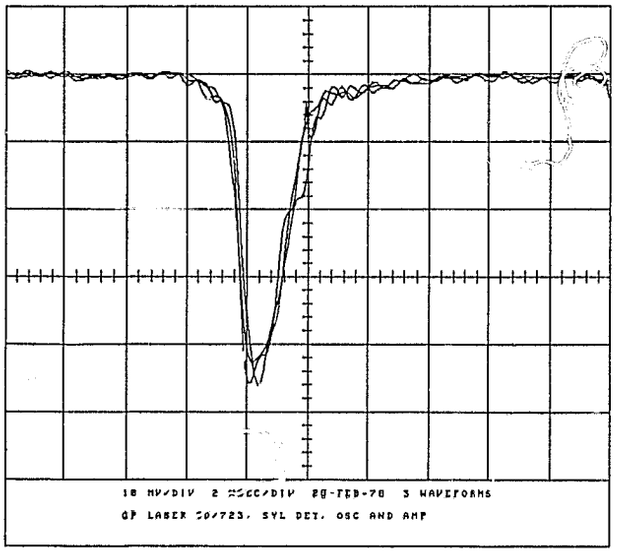

Figure 37(a). Several Output Pulse Profiles Obtained from the General Photonics Laser with the Government-supplied Krytron Cavity-dump Switch. The Pulsewidth is 1.5 Nanosecond between Half-maximum Points and 3.2 Nanoseconds between the 10% of Full Intensity Points.

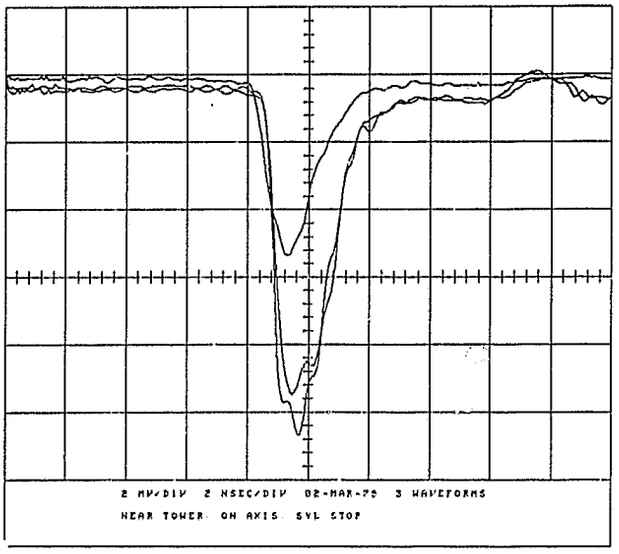

Figure 37(b). Several Waveforms Returned from the Tower when the Transmitter was Aligned On-axis (Zero Pointing Error).

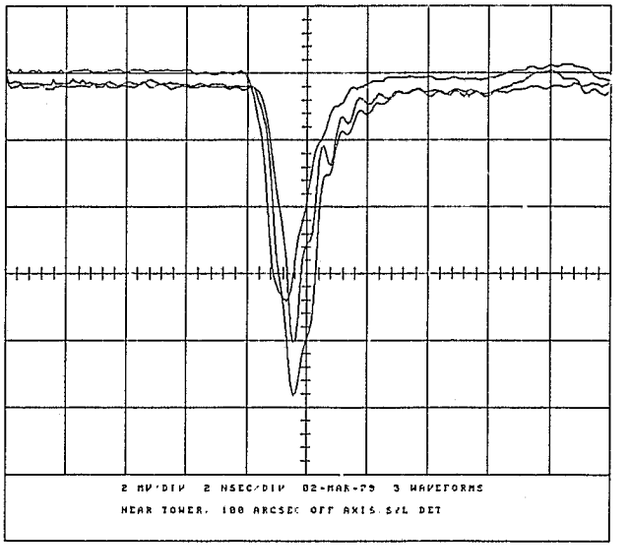

Figure 37(c). Several Waveforms Returning from the Tower Retroreflector when a 100 Arcsecond Pointing Error was Introduced into the Beam.

The total output energy from the double-pass amplifier was only about 60 mJ during the range measurements to be discussed. The frequency-doubled output at 5320Å was measured to be 15 millijoules.

During the time required to make the switch modifications, the Phase II receiver was reassembled and tested so that a direct comparison of the modified cavity-dumped transmitter with the earlier Q-switched versions would be possible. The electrically generated receiver time walk curves obtained before and after the cavity-dumped transmitter ranging tests are shown in Figures 38(a) and 38(b) respectively.

Stability measurements, using the cavity dumped transmitter and Phase II receiver on two consecutive days, are shown in Figures 39(a) and 39(b). On March 1, 1979, the peak-to-peak variation in the mean range was ±0.5 cms over a 90 minute time interval. The next morning, the peak-to-peak variation was less than ±1.5 cms over a two hour period. The RMS standard deviation in each 100 point data set was stable at about 2.5 cms. The shot-to-shot variation in a set of 250 consecutive range measurements is displayed in Fig. 40. This particularly good data set was taken on the same day as the repeatability data in Fig 39(a)and has a RMS standard deviation of only 1.1 cms.

Range maps were also made on the same days as the repeatability tests. Figs. 41(a) and 41(b) display the range map results obtained on March 1 and March 2 respectively. The maps show a peak-to-peak variation in the mean range of 3.55 cms (±1.78 cm) and 2.98 cms (±1.49 cms) on March 1 and 2 respectively. Assuming that all pointing angles are weighted equally, the RMS standard deviation in the mean range was only 0.73 cm and 0.72 cm on March 1 and 2 respectively. Clearly, the cavity-dumped laser significantly reduced the bias errors relative to the simple Q-switched system. A qualitative physical explanation for this improved performance is given in the next section.

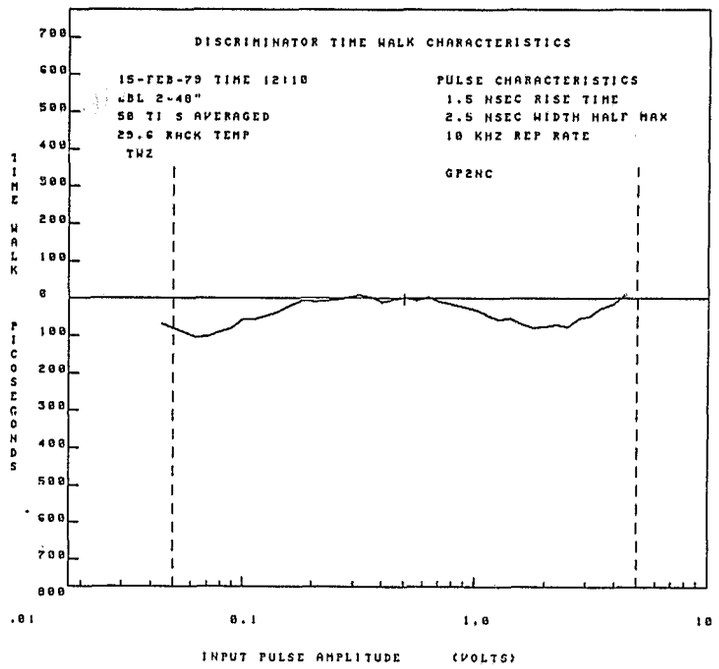

(a)

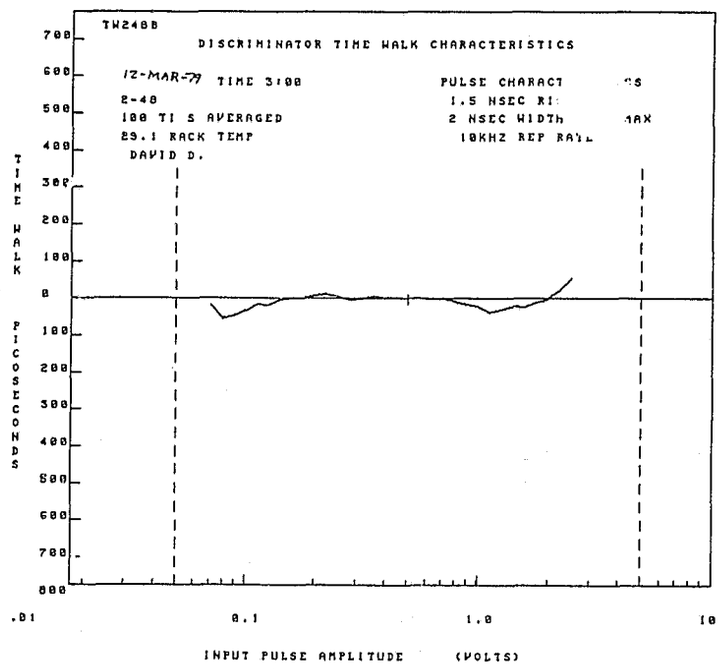

(b)

Figure 38. Receiver Time Walk Curves Obtained:
(a) Before the Final Ranging Test Sequence and
(b) After the Test Sequence.

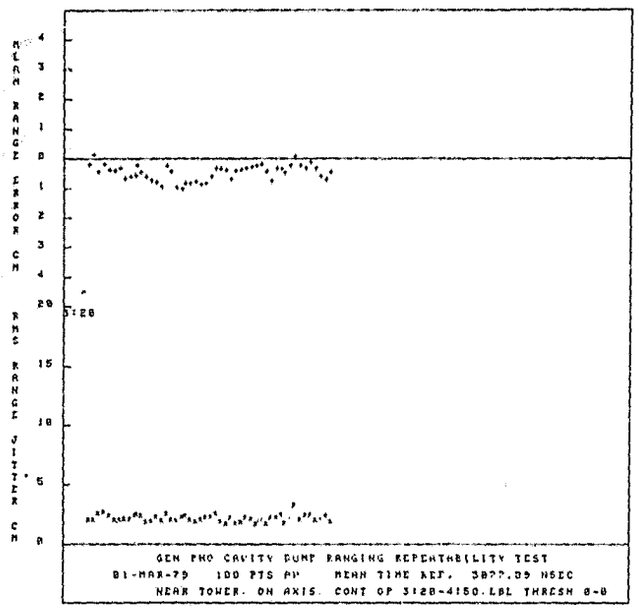

(a)

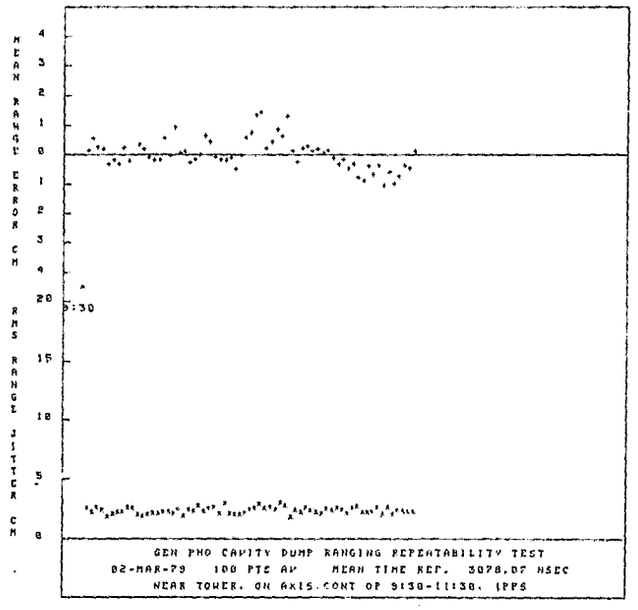

(b)

Figure 39. Results of the Repeatability Tests using the Phase II Ranging Receiver with the General Photonics Laser Cavity-dumped by the Government-supplied Krytron Switch. Each Mean Value Represents the Average over 100 Individual Range Measurements Relative to an Arbitrary Reference Value. The RMS Standard Deviation was stable at 2 to 3 cms.
(a) March 1, 1979 and (b) March 2, 1979.

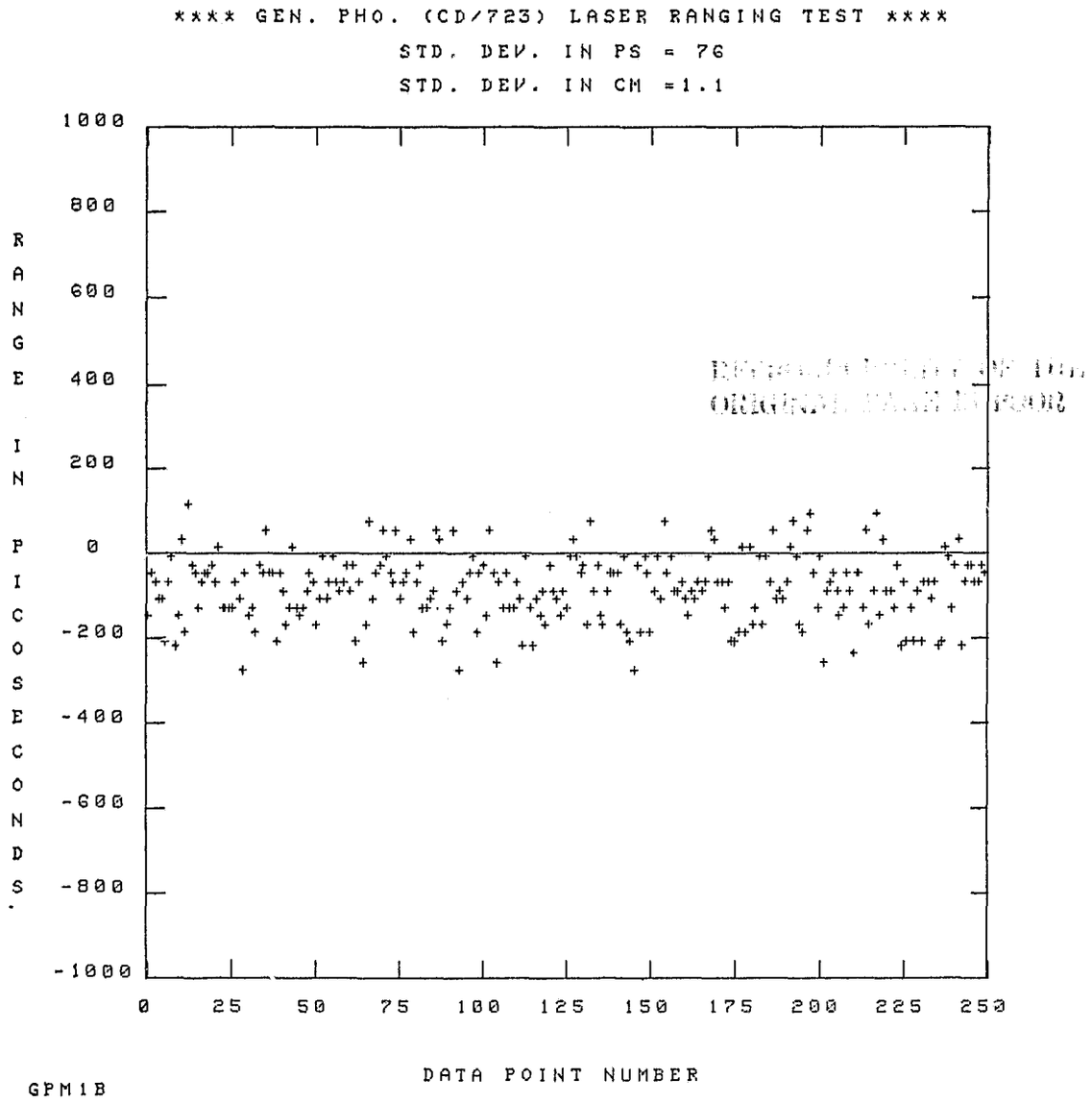

Figure 40. A Record of the Shot-to-shot Variations in the Time of Flight Measurements to the Tower Retroreflector.

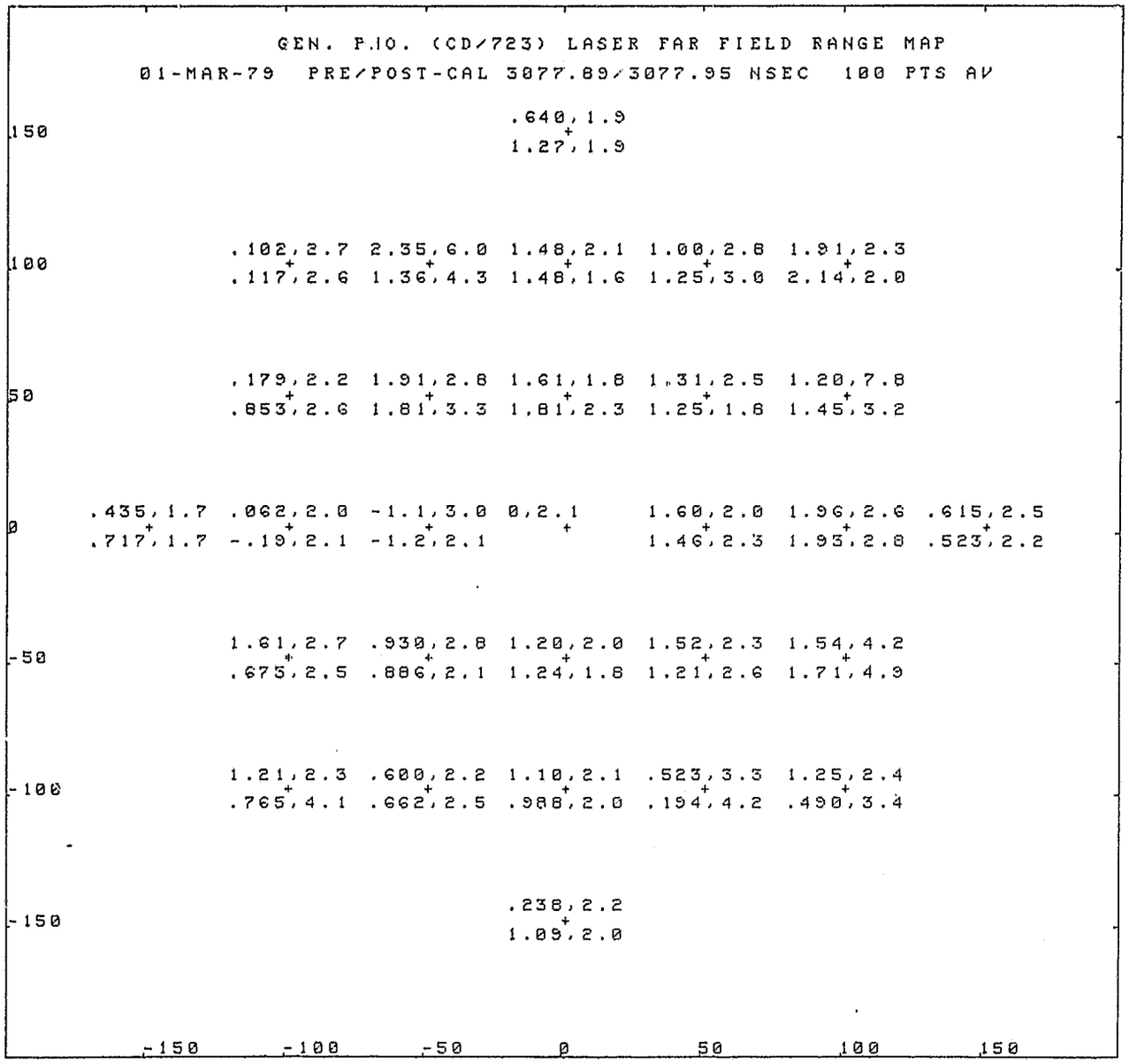

(a)

Figure 41. Results of a Range Map Taken with the Ranging System Consisting of the Phase II Receiver and the General Photonics Laser Cavity-dumped by the Government-supplied Krytron Switch. The First Number at Each Farfield Grid Point Corresponds to the Deviation of the Mean Value from the Reference Value in Centimeters while the Second Number Gives the RMS Standard Deviation About the Mean. Two Successive Measurements of 100 Data Points Each Were Made at Each Angular Setting. (a) March 1, 1979 and (b) March 2, 1979.

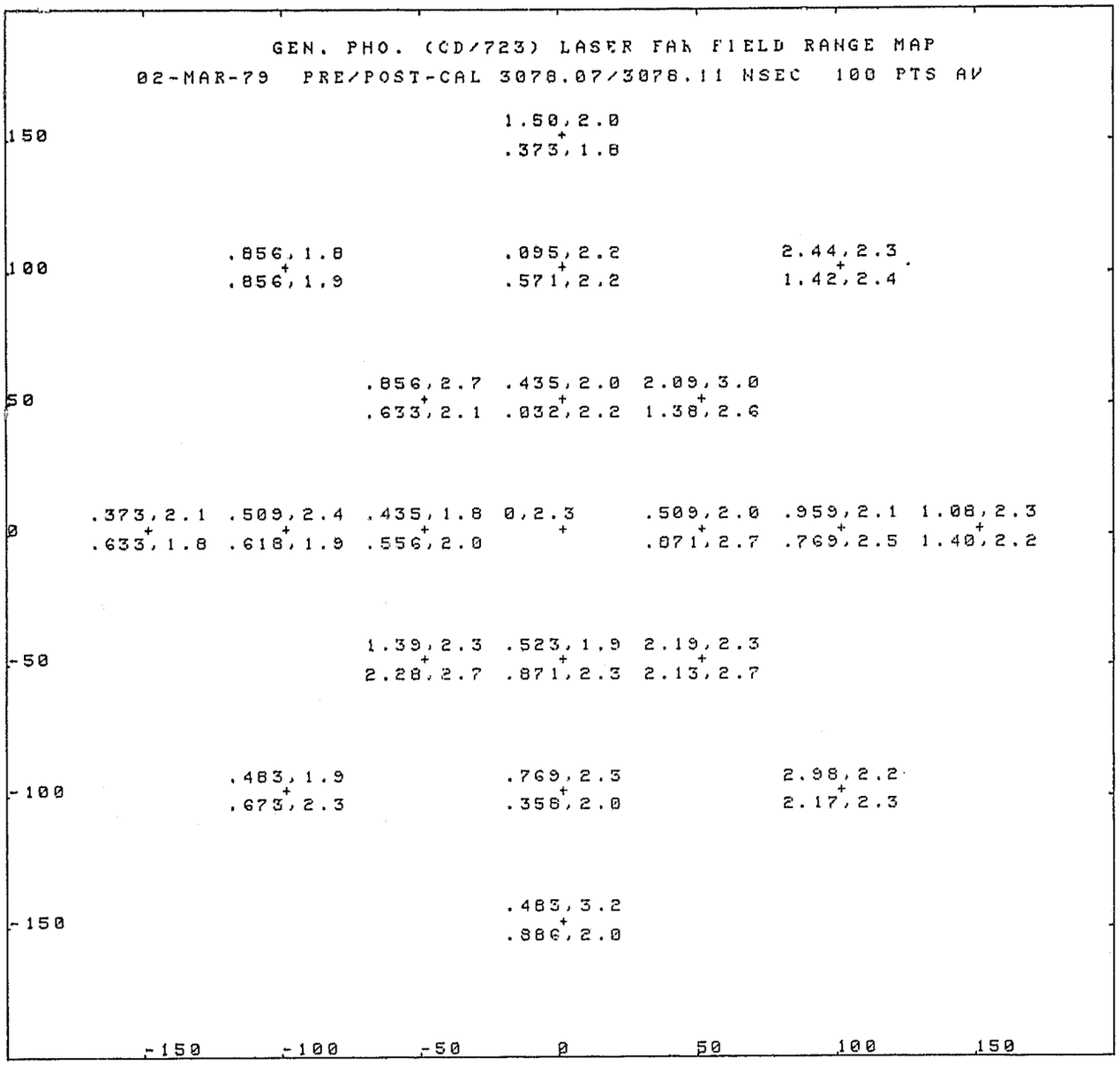

(b)

Figure 41 (Continued)

IX. Discussion

There are two processes taking place within the simple Q-switched version of the General Photonics Laser which degrade the ranging performance. The first of these is a tendency of the oscillator to modelock in a non-stationary manner. The effect can be represented as a comb of subnanosecond pulses with a relative spacing of approximately two nanoseconds (corresponding to the cavity round trip time) sliding back and forth in a random fashion within a four to six nanosecond (FWHM) pulse envelope. This behavior is the result of an interaction between different longitudinal modes of the laser. The second process is a random and uncontrolled buildup of different transverse modes which are allowed to leak out of the cavity at arbitrary times by the partially reflecting mirror. Because of their different antenna patterns,[5] the individual temporal profiles of the modes do not sum uniformly in the far field. As a result, the step waveform returning from the retroreflector may vary significantly from the start waveform leading to angularly dependent range biases. It is important to point out that longitudinal modelocking effects are not unique to the General Photonics Laser and, in fact, have been observed previously by us in Q-switched lasers provided by other manufacturers including International Lasers Systems and, to a lesser extent, a militarized Westinghouse unit. Higher order transverse mode operation is typical of most commercial Q-switched lasers which use "stable"[5] optical resonators.

From the previous discussion, one might conclude that the ideal Q-switched system for ranging applications would be a laser which operated in a single longitudinal mode and the lowest order transverse mode (TEM_{00} gaussian mode). Operation in a single longitudinal mode would require the introduction of frequency-dispersive elements in the cavity capable of discriminating between the different longitudinal modes which, in the General Photonics laser, are separated by only 500 MHz or .02Å. Multiple dispersive elements would be required to attain such a high spectral resolution, would greatly reduce the output energy of the oscillator, and would represent a major redesign effort. High power operation in a single transverse mode would require the use of internal beam expanders to increase the TEM_{00} mode volume. Such a modification would also increase the cavity length thereby leading to output pulses of longer duration. In addition, the differences in loss between the various longitudinal and transverse modes are small, and it requires many passes through the resonator at low gain

to make a single mode dominant. As a result, longitudinal and transverse mode selection has often been accomplished using prelase techniques.[6,7] For example, by applying a small voltage to the Q-switch, the laser is allowed to oscillate just above threshold for a relatively long period of time. At the end of this prelase period, the system is fully Q-switched for maximum energy extraction. Similar behavior can be obtained by the use of a slow saturable absorber, such as a Q-switching dye, in place of the electro-optic switch.

The experimental results at the end of Section VII indicate that single transverse mode operation without single longitudinal mode operation will not improve the ranging performance of a simple Q-switched transmitter. In light of the practical difficulties in achieving simultaneous single transverse and single longitudinal mode operation in a Q-switched laser and the major redesign effort involved, this course is not recommended. Furthermore, the Phase III tests confirmed that cavity-dumping the oscillator can reduce the transmitter bias errors to the centimeter level. The latter is a relatively simple modification to implement and minimizes the redesign effort.

It was mentioned in the Introduction that similar poor results had been obtained with the earlier Q-switched ruby systems and that the incorporation of a cavity-dump greatly improved the ranging performance of these lasers. Q-switched and cavity dumped lasers, sometimes referred to as Pulse Transmission Mode (PTM) Q-switched lasers, are physically similar to the simpler Q-switched systems but their operation is somewhat different as outlined in Fig. 42. In both types of systems, a quarter-wave voltage applied to the Pockels cell will prevent the cavity from oscillating during the "hold-off" period during which the population inversion is building to a maximum near the end of the flashlamp emission.

Upon reaching maximum gain, the Q-switch command is given and the Pockels cell transmission goes to unity. At this point, the cavity sees a net gain and the radiation intensity builds up within the cavity.

The radiation envelope is the sum of the intensities in each individual laser mode. When mode beating effects are present, the internal radiation is modulated with a period corresponding to the

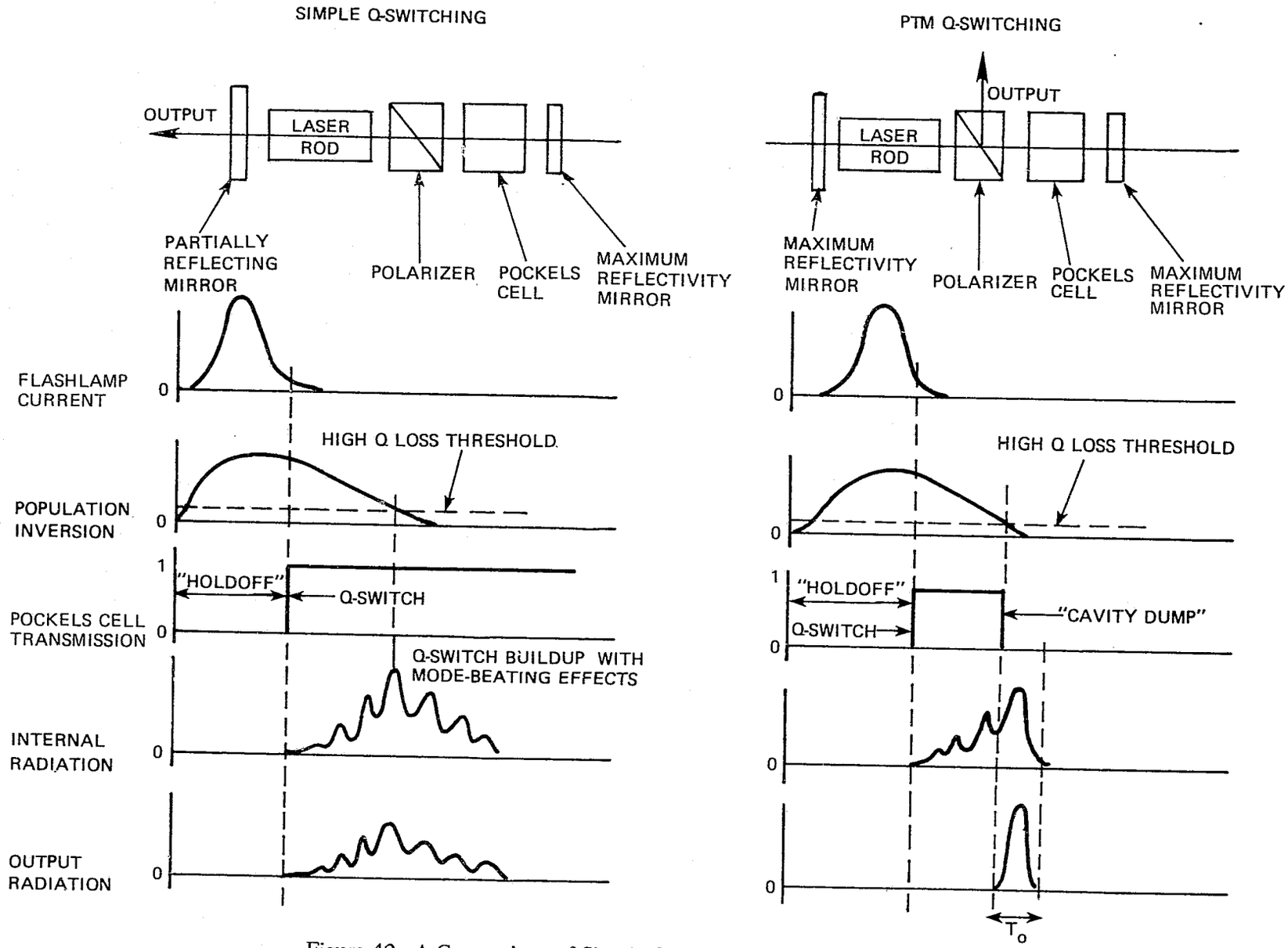

Figure 42. A Comparison of Simple Q-switching and PTM Q-switching

roundtrip cavity transit time. In actual fact, the pulse train in Fig. 42 is really a single pulse circulating in the cavity. In the simple Q-switched system, a constant fraction of the circulating pulse energy is coupled out by the partially reflecting mirror and hence the laser output is also modulated. When the laser gain equals the residual loss threshold of the high Q-oscillator, the circulating pulse is no longer amplified and the pulse amplitude decays with time.

In the cavity dump system, no radiation is permitted to leave the resonator due to the presence of two maximum reflectivity mirrors. When the Q-switched radiation reaches a maximum inside the cavity (as determined by monitoring low-level radiation leakage through the end mirrors), the Pockels cell transmission is again returned to zero by application of a quarter-wave voltage across the cell. The polarization of the circulating radiation is then rotated by 90° by a two-way transit through the cell, and the circulating energy is ejected from the cell by the polarizer. For the ideal case of an infinitely fast switch, all of the internal radiation is dumped from the cavity within a single roundtrip cavity transit time, T_o. In practical systems, finite switching speeds on the order of a nanosecond result in somewhat longer output pulses. While cavity-dumped oscillators do not prevent the simultaneous buildup of different longitudinal and transverse modes, they do minimize their effects on ranging by ejecting all of the modes from the cavity during a very narrow time interval corresponding roughly to the roundtrip cavity time. Thus, in principle at least, the circulating pulse is totally ejected from the cavity and a single unmodulated output pulse is observed. In practice, however, finite switching speeds and imperfect polarization extinction ratios can allow some temporal modulation of the ejected pulse. The steep leading edge, short pulsewidth, and relatively unmodulated character of the pulse waveforms in Fig. 37 is a good indication that subnanosecond switching speeds are being obtained with the inhouse krytron switch.

In conclusion, we strongly recommend that the present MOBLAS systems be modified to incorporate a fast cavity dump switch in the oscillator. Krytron and avalanche transistor chains are both capable of achieving the necessary switching speeds. It is anticipated that, in order to obtain maximum reliability and ranging performance from the oscillator, some reduction in the final output

energy may be necessary. This can be compensated for, if necessary, by the inclusion of a second amplifier. The shorter pulsewidth will also result in improved doubling efficiencies.

Acknowledgments

The authors are grateful to H. Edward Rowe and Robert Appler for their technical assistance throughout the testing period, to James B. Abshire for his assistance in optimizing the receiver, and to Bernard J. Klein who performed the laser geodemeter measurements. Modification of the cavity dump switch was carried out by Thomas S. Johnson and Jeffrey Lessner. The authors also wish to thank Thomas E. McGunigal and Dr. Michael W. Fitzmaurice for helpful discussions on various aspects of laser ranging. David Douglas performed the Phase III discriminator time walk tests.

REFERENCES

1. T. E. McGunigal, W. J. Carrion, L. O. Caudill, C. R. Grant, T. S. Johnson, D. A. Premo, P. L. Spadin and G. C. Winston, "Satellite Laser Ranging Work at the Goddard Space Flight Center," TMS-723-75-172, July 1975.
2. J. B. Abshire, T. W. Zagwodzki, "Advanced Laser Ranging Receiver Development," NASA X-723-78-22, July 1978.
3. T. W. Zagwodzki, "Testing and Evaluation of a State-of-the-Art Time Interval Unit," NASA X-723-77-290, December 1977.
4. G. A. Schnelzer, "A Comparison of Atmospheric Refractive Index Adjustments for Laser Satellite Ranging," Hawaii Institute of Geophysics Report HIG-72-14, Sept. 1972.
5. H. Kogelnik and T. Li, "Laser Beams and Resonators," Applied Optics, Vol. 5, pp. 1550-1567 (Oct. 1966).
6. J. M. McMahon, "Laser Mode Selection with Slowly Opened Q-switches," IEEE J. Quantum Electronics, QE-5, P. 489-495 (Oct. 1969).
7. V. Daneu, C. A. Sacchi and D. Svelto, "Single Transverse and Longitudinal Mode Q-switched Ruby Laser," IEEE J. Quantum Electronics, QE-2 pp. 290-293 (August, 1966).

8. J. B. Abshire, "Characterization of a Maximum Likelihood Laser Ranging Receiver," to be published.

9. T. S. Johnson and J. Lessner, Unpublished.

BIBLIOGRAPHIC DATA SHEET

1. Report No. TM80336	2. Government Accession No.	3. Recipient's Catalog No.
4. Title and Subtitle Characterization of the Q-Switched Moblas Laser Transmitter and its Ranging Performance Relative to a PTM Q-Switched System		5. Report Date October, 1979 6. Performing Organization Code 723
7. Author(s) John J. Degnan, Thomas W. Zagwodzki		8. Performing Organization Report No.
9. Performing Organization Name and Address Instrument Electro-Optics Branch, Code 723 Goddard Space Flight Center Greenbelt, Maryland 20771		10. Work Unit No. 11. Contract or Grant No. 13. Type of Report and Period Covered Technical Memorandum
12. Sponsoring Agency Name and Address Goddard Space Flight Center Greenbelt, Maryland 20771		14. Sponsoring Agency Code

15. Supplementary Notes

16. Abstract

A prototype Q-switched Nd:YAG laser transmitter intended for use in the NASA mobile laser (MOBLAS) ranging system was subjected to various tests of temporal pulse shape and stability, output energy and stability, beam divergence, and range bias errors. Peak-to-peak variations in the mean range were as large as 30 cm (±15cm) and drift rates of system bias with time as large as 6mm per minute of operation were observed. The incorporation of a fast electro-optic cavity dump into the oscillator gave significantly improved results. Reevaluation of the ranging performance after modification showed a reduction in the peak-to-peak variation in the mean range to the 2 or 3 cm level and a drift rate of system time biases of less than 1 mm per minute of operation. A qualitative physical explanation for the superior performance of cavity dumped lasers is given.

17. Key Words (Selected by Author(s))	18. Distribution Statement
Nd:YAG Laser, Laser Ranging Q-Switched, Cavity Dumped	

19. Security Classif. (of this report)	20. Security Classif. (of this page)	21. No. of Pages	22. Price*
UNCLASSIFIED	UNCLASSIFIED	75	

*For sale by the National Technical Information Service, Springfield, Virginia 22151.